Chebyshev tau - QZ Algorithm Methods for Calculating Spectra of Hydrodynamic Stability Problems*

J.J. Dongarra(1), B. Straughan(2) ** & D.W. Walker(2)

(1)Department of Computer Science, University of Tennessee, Knoxville, Tennessee 37996-1301, U.S.A., and Mathematical Sciences Section, Computer Science and Mathematics Division, Oak Ridge National Laboratory, P.O. Box 2008, Oak Ridge, Tennessee 37831 - 6367, U.S.A.

(2)Mathematical Sciences Section, Computer Science and Mathematics Division, Oak Ridge National Laboratory, P.O. Box 2008, Oak Ridge, Tennessee 37831 - 6367, U.S.A.

Abstract

The Chebyshev tau method is examined in detail for a variety of eigenvalue problems arising in hydrodynamic stability studies, particularly those of Orr-Sommerfeld type. We concentrate on determining the whole of the top end of the spectrum in parameter ranges beyond those often explored. The method employing a Chebyshev representation of the fourth derivative operator, D^4, is compared with those involving the second and first derivative operators, D^2, D, respectively; the latter two representations require use of the QZ algorithm in the resolution of the singular generalised matrix eigenvalue problem which arises. The D^2 method is shown to be different from the stream function - vorticity scheme in certain (important and practical) cases. Physical problems explored are those of Poiseuille, Couette, and pressure gradient driven circular pipe flow. Also investigated are the three-dimensional problem of Poiseuille flow arising from a normal velocity - normal vorticity interaction, and finally Couette and Poiseuille problems for two viscous, immiscible fluids, one overlying the other are studied.

Keywords: Eigenvalue problems, Orr-Sommerfeld equations, Multi-layer flows, Chebyshev polynomials, QZ algorithm.

---

* This work was supported in part by the Office of Scientific Computing, U.S. Department of Energy under contract DE-AC05-84OR21400 with Lockheed Martin Energy Systems, and by the Advanced Research Projects Agency under contract DAAL03-91-C-0047, administered by the Army Research Office.

** Permanent address: Department of Mathematics, The University, Glasgow, G12 8QW, U.K.

1. Introduction

There has been much recent attention directed at solving equations like the Orr - Sommerfeld one, with particular interest in the removal of spurious eigenvalues or calculations in high Reynolds number ranges, cf. Abdullah & Lindsay [1], Davey [7], Fearn [12], Gardner *et al.* [13], Huang & Sloan [20], Lindsay & Ogden [21], McFadden *et al.* [22], Orszag [27], and Zebib [40]. Equations of Orr-Sommerfeld type govern the stability of shear and related flows which have tremendous application in many fields. One such field is climate modelling with questions like determining an explanation for the origin of the mid-latitude cyclone which in turn is responsible for producing the high and low pressure regions from which variable weather patterns arise. Another application is to shear flows in electrohydrodynamic (EHD) systems which have industrial relevance in the invention of devices employing the electroviscous effect or those utilizing charge entrainment, such as EHD clutch development, or EHD high voltage generators. Yet other important mundane applications include the prediction of landslides, and flow over an aeroplane wing covered in de-icer. These topics will form part of future research.

Of especial interest to the present contribution is the paper by McFadden *et al.* [22]. These writers propose a modified Chebyshev tau method which involves setting to zero two columns of the B matrix in the generalised eigenvalue problem

$$A\mathbf{x} = \sigma B\mathbf{x}, \tag{1.1}$$

which arises from a representation of a solution to the differential equation by a finite series of Chebyshev polynomials. At first sight this may seem ad hoc; however, [22] provides an elegant proof of why their technique is equivalent to a stream function - vorticity scheme, at least for the modified problem studied there. Our goal is to investigate in detail a method which for many two-dimensional problems is equivalent to the stream function - vorticity method of McFadden *et al.* [22]. The technique employed here also extends to practical three - dimensional stability problems for which a stream function - vorticity formulation is not so clear. The motivation for requiring a technique involving only second order derivatives is that this involves matrices whose coefficients grow at most $O(M^3)$, M being the number of Chebyshev polynomials; since we study Couette / Poiseuille type problems in high Reynolds number regimes we require many polynomials and then it is vital to avoid round off error due to growth of terms. In fact, we highlight three types of error one can expect to find in Couette / Poiseuille flow stability calculations and ramifications of these. It is shown how to modify the method to deal with these errors. We apply the method to obtain new results for a variety of interesting shear flow / pressure gradient driven hydrodynamic stability problems.

To begin our discussion we shall consider the Orr-Sommerfeld equation

$$(D^2-a^2)^2\phi = iaRe(U-c)(D^2-a^2)\phi - iaReU''\phi, \qquad z\in(-1,1), \tag{1.2}$$

see Drazin & Reid [11], equation (25.12), where $D=d/dz$, Re, a and c are Reynolds number, wavenumber, and eigenvalue (growth rate), respectively, and ϕ is the amplitude of the stream function. For Poiseuille flow $U=1-z^2$, whereas for Couette flow $U=z$. Equation (1.2) is solved subject to the boundary conditions

$$\phi = D\phi = 0, \qquad z=\pm 1. \tag{1.3}$$

To motivate what follows a brief description of the fluid dynamics behind equation (1.2) is expedient. This equation arises in a study of linear instability of the flow of a fluid contained between infinite parallel plates at $z=\pm1$, which are sheared relative to one another (Couette flow) or the fluid is driven by a pressure gradient in the horizontal direction (Poiseuille flow). If the components of perturbation velocity and pressure are (u,v,w,p) then the differential equations for these variables are, cf. Drazin & Reid [11], p. 128,

$$\begin{aligned}(ReU-c)iau+ReU'w &= -\,iap+\big(D^2-[a^2+b^2]\big)u,\\ (ReU-c)iav &= -\,ibp+\big(D^2-[a^2+b^2]\big)v,\\ (ReU-c)iaw &= -\,Dp+\big(D^2-[a^2+b^2]\big)w,\\ iau+ibv+Dw &= 0,\end{aligned} \tag{1.4}$$

where a and b are horizontal wavenumbers in the x and y directions and equations (1.4) arise from a representation like

$$u_i = u_i(z)e^{i(ax+by-act)}, \qquad p=p(z)e^{i(ax+by-act)}, \tag{1.5}$$

with $u_1=u, u_2=v, u_3=w$. Traditional thinking has argued that the transformations

$$Re\to \tilde{Re}\,\frac{\tilde a}{a}, \qquad c\to \tilde c\,\frac{\tilde a}{a},$$

reduce (1.4) to a two-dimensional form (Squire's theorem)

$$\begin{aligned}(ReU-c)iau+ReU'w &= -\,iap+(D^2-a^2)u,\\ (ReU-c)iaw &= -\,Dp+(D^2-a^2)w,\\ iau+Dw &= 0.\end{aligned} \tag{1.6}$$

The boundary conditions are $u=w=0$ on $z=\pm1$ and then by introduction of a stream function ψ with

$$u=\frac{\partial\psi}{\partial z}, \qquad w=-\frac{\partial\psi}{\partial x},$$

and writing

$$\psi = \phi(z)e^{ia(x-ct)},$$

one derives (1.2), (1.3) for the solution to the instability problem.

A recent school of thought has challenged traditional thinking and argued that since experiments predict instabilities earlier than the critical value of linear theory then the true situation may be a three-dimensional one where resonances between individual modes can lead to very large transient growth over a small time scale, and after that presumably nonlinear effects become important. The early resonance investigations are by Gustavsson [14] and Gustavsson & Hultgren [15], and much activity has followed, see e.g. Butler & Farrell [3], Henningson & Reddy [17], Reddy & Henningson [28], Reddy *et al.* [29], Schmid & Henningson [32], Shanthini [33], and Trefethen *et al.* [38], and the references therein.

The particular reason why we are interested in the above works is that we have investigated a Chebyshev tau method which reduces the fourth order equation to two second order ones, as do Gardner *et al.* [13], and the stream function - vorticity method of McFadden *et al.* [22]. Our premise is that the method involving only second derivatives is much better for accurate results because the growth of terms in the A matrix in (1.1) is considerably less. Further details are provided below.

The fundamental paper of Orszag [27] solves (1.2), (1.3) by a Chebyshev tau method to high accuracy and we make comparison with his work. He splits the problem into odd and even modes which is best if one knows *a priori* this can be done. For the most part we deal directly with (1.2), (1.3) since this would allow the incorporation of effects such as penetrative convection into the fluid dynamics.

One method to solve (1.2), (1.3) directly is as in Gardner *et al.* [13] section 2, whereby one writes

$$\phi = \sum_{n=0}^{N+4} \phi_n T_n(z),$$

and removes the boundary condition columns from the Chebyshev representation of D^4. This we have done taking care to employ the Herbert [18] form of representation of coefficients in D^4, cf. Canuto *et al.* [4] p. 196, since this leads to smaller round off error. If we put $M = N + 1$, then for M large, the matrix resulting from D^4 has terms growing like $O(M^7)$ and since for high Reynolds number calculations a large number of polynomials are required (possibly at least 200) this can be a serious problem. This is one immediate reason for preferring a method involving D^2, since then the growth is only $O(M^3)$. Gardner *et al.* [13] do develop a D^2 method for the Orr-Sommerfeld equation; due to the way they remove boundary condition rows, the growth problem is still present. Their technique still has $O(M^6)$ growth due to the B_1Q term in their equation (3.9b); B_1 and Q each involve

$\chi_2 F_2$ (in their notation) and this term is like $O(M^3)$, and so the modified tau method of Gardner *et al.* [13] still does not remove the growth problem.

A D^2 method writes (1.2) as two equations

$$\begin{aligned}&(D^2-a^2)\phi - A = 0,\\ &(D^2-a^2)A - iaRe(U-c)A + iaReU''\phi = 0.\end{aligned}$$

The difficulty with doing this, as pointed out by McFadden *et al.* [22], p. 232, is that the boundary conditions are all on ϕ and none are on A. Thus, we cannot remove boundary condition rows by the Haidvogel - Zang [16] device. (If the boundary conditions are those appropriate to surfaces free of tangential stress then there are two boundary conditions on ϕ and two on A and one can remove the offending boundary condition rows. This we have done for Orr-Sommerfeld problems, and in a practical multi-component diffusion problem involving penetrative convection; we obtain highly accurate results and no spurious eigenvalues, see Straughan & Walker [37]. Also, for porous convection problems the natural boundary conditions allow boundary condition removal in the A matrix and very satisfactory results are yielded, Straughan & Walker [35,36].)

Instead we try the heuristic approach of simply writing in the boundary conditions as rows of the matrix, cf. McFadden *et al.* [22], p. 232. This is also done by Lindsay & Ogden [21] who generalized the Gardner *et al.* [13] method and solved (1.2), (1.3) as a system of four first order equations; we refer to their technique as a D-method. As we have pointed out in Straughan & Walker [36] when we use the Lindsay & Ogden [21] technique on the simple harmonic motion equation with homogeneous boundary conditions we detect a spurious eigenvalue; this feature persists even if we use a symmetric form of boundary conditions. Also, both the D^2 and D methods are *ad hoc* in that one has some freedom as to how to insert the boundary conditions; we have found that a symmetric form of boundary conditions is preferable for the Orr-Sommerfeld equations.

A D^2-method for (1.2), (1.3) appropriate to Poiseuille flow solves an equation like (1.1) where

$$\mathbf{x} = (\phi_0, \ldots, \phi_N, \psi_0, \ldots, \psi_N)^T,$$

with

$$A_r = \begin{pmatrix} D^2-a^2I & -I \\ BC1 & 0\ldots0 \\ BC2 & 0\ldots0 \\ & \\ 0 & D^2-a^2I \\ BC3 & 0\ldots0 \\ BC4 & 0\ldots0 \end{pmatrix}, \qquad A_i = \begin{pmatrix} 0 & 0 \\ 0\ldots0 & 0\ldots0 \\ 0\ldots0 & 0\ldots0 \\ & \\ -2aReI & aRe(P-I) \\ 0\ldots0 & 0\ldots0 \\ 0\ldots0 & 0\ldots0 \end{pmatrix}$$

and

$$B_r = \mathbf{0}, \qquad B_i = \begin{pmatrix} 0 & 0 \\ & \\ 0 & -aReI \\ & 0\ldots0 \\ & 0\ldots0 \end{pmatrix}$$

where P is the Chebyshev matrix representing z^2, $A = A_r + iA_i$, and $B = B_r + iB_i$.

The rows $BC1, \ldots, BC4$ refer to the boundary conditions on ϕ_n and for the Orr-Sommerfeld problem we find it preferable to use the symmetric form given by Orszag [27] i.e. $BC1$, $BC2$ are $(15)_1$ and $(15)_2$ of Orszag [27] while $BC3, BC4$ are $(16)_1$, $(16)_2$ of the same paper.

In the two-dimensional case the D^2 method is simply the stream function - vorticity technique of McFadden *et al.* [22]. For, in that case, the vorticity has only one component, in the y-direction, $\omega = \omega_2$ with

$$\begin{aligned} \omega =& u_{,z} - w_{,x} \\ =& \psi_{,zz} + \psi_{,xx} \\ =& e^{ia(x-ct)}(D^2 - a^2)\phi. \end{aligned}$$

Thus the functions ϕ and A are essentially ψ and ω. We stress though that we are using the McFadden *et al.* [22] stream function - vorticity method (called here a D^2 method) because the resulting A matrix in (1.1) has better growth properties.

It is noteworthy though that the D^2 method is more general than the stream function - vorticity method. For example, in section 5 we consider the Butler & Farrell [3] problem which results in a coupled system involving a fourth order equation for w and a second order equation for the normal vorticity $\omega_3 = v_{,x} - u_{,y}$. In this three-dimensional situation we still reduce things to three second order equations and use a D^2 method which is then not equivalent to the usual stream function - vorticity method. Other areas where it differs are in three-dimensional convection studies in anisotropic porous media where the principal axes of the permeability tensor are not orthogonal to the layer, or the Hadley flow problem, see Straughan & Walker [35,36], respectively.

In the remainder of the paper we make a systematic study of Chebyshev tau methods applied to Poiseuille flow, Couette flow, Hagen-Poiseuille flow, the normal velocity - normal vorticity eigenvalue problem of Butler & Farrell [3], and finally we show how to apply the method to the situation where one fluid is overlying another. We stress that we concentrate on finding the whole of the top end of the spectrum, including eigenvalues at the "branch points" which are difficult to obtain, [27], and we investigate parameter ranges which have previously proved difficult. Consideration is given to loss of accuracy due to the various

D^4, D^2 or D methods, and to loss of accuracy due to insufficient polynomials, or insufficient resolution due to lack of precision in the representation of real numbers; each of these has a strong effect on the spectrum. The calculation of the spectrum is very important when one is interested in the question of resonances and interactions between various lower order modes, and it is vital when mode crossing occurs, as it does in practical problems.

2. The eigenvalue problem for plane Poiseuille flow

In this section we study (1.2), (1.3) with $U = 1 - z^2$. There have been many calculations of the spectral behaviour for Re not too large, say $Re \leq 10^4$, see Butler & Farrell [3], Drazin & Reid [11], Gustavsson [14], Henningson & Reddy [17], Mack [23], Orszag [27], Reddy & Henningson [28], Shanthini [33]. Abdullah & Lindsay [1], Davey [7] and Fearn [12] report studies on particular eigenvalues for Re extending to 10^9. We, therefore, use the D^2 (stream function - vorticity) method and show what can go wrong in calculating the spectrum for large Re and how one can put things right.

We have written our own codes for the D^4, D^2 and D methods, employing various forms of the boundary conditions in the latter two, including two forms of symmetric boundary conditions in the D method, one using Orszag's boundary conditions on ϕ directly, the other employing expressions like $(15)_1, (16)_1$ of Orszag [27] on both ϕ and ϕ' individually. A comparison of results for these methods is now given.

Undoubtedly the advantage of the D^2 method is the growth rate removal, and in this respect the D method is even better, with terms growing only like $O(M)$; this important feature does not appear to have been realised in Lindsay & Ogden [21]. Against this, the time taken by the QZ algorithm appears to scale like $O(M_{\text{size}}^3)$ where M_{size} is the matrix width, i.e. $M_{\text{size}} = M, 2M, 4M$, with the D^4, D^2, D methods, respectively; the problems associated with doubling the matrix size have been commented on by McFadden *et al.* [22]. For example, on a SUN sparc station (ipc), with 50 polynomials, the D^4, D^2, D methods take, respectively, 4.1 seconds, 17.1 seconds, and 112.3 seconds. One test of the D method with $M = 150$ took 2940.7 seconds, i.e. approximately 49 minutes. Clearly, when many computations are required this is an important factor. Additionally, the memory requirements of the D method are substantial, requiring approximately 16MB for the 150 polynomial case (using full precision). The D^2 method we have found to yield high accuracy, although as reported below, for Re high enough extended precision arithmetic is required. Unless explicitly stated, our calculations are based on full precision, i.e. 64 bit, arithmetic.

The D^2 and D methods necessarily produce a B matrix in (1.1) which has one or more rows of blocks of 0's and so is singular. One approach to solving this problem is the QZ algorithm of Moler & Stewart [25]. This algorithm relies on the fact that there exist unitary matrices Q and Z such that QAZ and QBZ are both upper triangular. The algorithm then yields sets of values α_i, β_i which are the diagonal elements of QAZ and QBZ. The eigenvalues σ_i of (1.1) are then obtained from the relation $\sigma_i = \alpha_i/\beta_i$, provided $\beta_i \neq 0$. This is very important, since the way we have constructed B means it contains a singular band, corresponding to infinite eigenvalues, and the $\beta_i = 0$ must be filtered out. Indeed, with the technique advocated here one ought always to consider the α_i and β_i, since as Moler & Stewart [25] point out, the α_i and β_i contain more information than the eigenvalues themselves. The QZ algorithm is available in the routines ZGGHRD, ZHGEQZ and ZTGEVC of the LAPACK Fortran Subroutine library, Anderson *et al.* [2]. The coefficients of the eigenvector $\mathbf{x}$ yielded by the QZ algorithm are extremely useful convergence indicators. In fact, they can be used to indicate the presence of spurious eigenvalues; the "eigenvector" for such a spurious eigenvalue typically does not demonstrate the convergence evident in the eigenvector for a real eigenvalue. An alternative way is to compute the τ - coefficients, cf. Gardner *et al.* [13], but as these are based on the eigenvector we find it simpler to just examine the eigenvectors themselves. Another possible method of assessing whether an eigenvector is spurious is to compute the residuals for (1.1), i.e. compute

$$\mathbf{r}^{(i)} = \beta_i A\mathbf{x}^{(i)} - \alpha_i B\mathbf{x}^{(i)}.$$

When an eigenvalue is spurious we have found these to have *all* components between $O(10^{22})$ and $O(10^{18})$. For a real eigenvalue, the residuals corresponding to those $\beta_i = 0$ are $O(10^{18})$ as are two or three corresponding to the presence of spurious eigenvalues, whereas the rest converge from $O(10^6)$ down to $O(10^{-8})$, which is consistent with the fact that the discretization only allows us to see the "top end" of the true spectrum. Even though we are using a D^2 method we do find a spurious eigenvalue may be produced; when we apply the method to the problem of two fluids in section 6 then we always see spurious eigenvalues. In connection with this, we have calculated the sensitivities for the eigenvector, cf. Stewart & Sun [34], and these indicate that the spurious eigenvalues are connected with the discretization procedure rather than the QZ algorithm used to find the matrix eigenvalues; details appropriate to the superposed fluid problem are given in section 6.

Orszag [27] gives for $Re = 10^4$ and $a = 1$,

$$c = 0.23752649 + 0.00373967i \tag{2.1}$$

as the exact value of the first eigenvalue (to 8 d.p.); he used 56 polynomials to achieve this accuracy (although he only uses even ones, thereby only 28 terms are in his expansion). The D^4 method gives

$$c = 0.23752708 + 0.00373980i$$

with $M = 50$. We found this to be the best approximation and thereafter on increasing M the value diverges from (2.1). The D^2 and D methods, however, agree with (2.1) for $M = 56$ and beyond. We can also find the eigenfunctions very accurately; for example, the D^2 method with 56 polynomials yields ϕ_r and ϕ_i as in figure 4.20 of Drazin & Reid [11]. In the symmetric versions of the D^2 and D methods we obtained only even modes for cases when the eigenfunction is symmetric and odd modes in the skew symmetric case, and the convergence is better than that for the D^4 technique. Another feature of the D^4 method is that even though the boundary conditions are removed we still saw two values in the list with $\beta = 0$; the corresponding α values were large, $O(10^{15})$, and real. These we believe are spurious but are easily filtered out by examining the β_i given by the QZ algorithm.

Orszag [27] table 5 gives a list of the 32 least stable modes for $Re = 10^4$, $a = 1$. With the D^2 method we obtained complete agreement with this list in the sense: for the first 12 eigenvalues with 70 polynomials, for the first 14 eigenvalues with 80 polynomials, and complete agreement with all 32 eigenvalues by using 96 polynomials. We did, however, find an extra eigenvalue; between positions 17 and 18 of Orszag [27] table 5 we obtain the value

$$c = 0.21272578 - 0.19936069i. \tag{2.2}$$

The eigenvector coefficients from the D^2 method with 96 polynomials indicate the value (2.2) corresponds to a skew-symmetric solution and with this number of polynomials the eigenvector had converged to $O(10^{-13}), O(10^{-14})$, for the ϕ and A $(= D^2\phi - a^2\phi)$ terms. Interestingly, we find both symmetric and skew symmetric modes with the D (and D^2) method(s); Lindsay & Ogden [21] appear to report only symmetric ones. For $Re = 10^4, a = 1$, the spectrum, in the range $c_i \in (-1, 0)$, $c_r \in (0, 1)$, is given in figure 1, indicating which are even and which are odd modes. When we refer to the spectrum in a figure here and throughout the paper we mean that part displayed in the relevant figure.

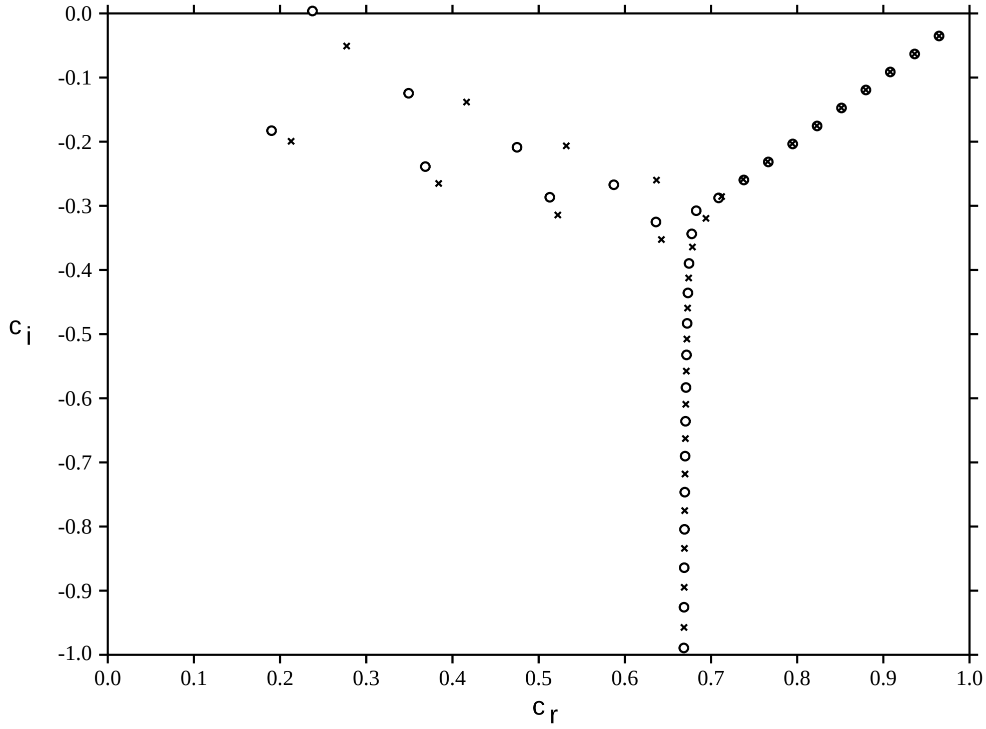

Figure 1 The spectrum for plane Poiseuille flow. $Re = 10^4, a = 1$, open circle ($\circ$) = even eigenfunction, cross ($\times$) = odd eigenfunction. The upper right branch consists of "degenerate" pairs of even and odd eigenvalues.

We have produced an mpeg movie which may be accessed with a web browser, such as Mosaic or Netscape, at

`http://www.epm.ornl.gov/~walker/eigenproblems.html`

This movie contains the parametric evolution of the spectrum of the plane Poiseuille flow problem for $a = 1$, with Re ranging from 100 to 10^4 in steps of 10. This may yield useful insight into resonance mechanisms. The evolution of the upper branches is clearly visible and the emanence of the eigenvalues from $c_r = 2/3$ is evident.

When Re is increased eventually mode crossing is seen, i.e. eigenvalues exchange positions in the sense that the imaginary part of one eigenvalue decreases relative to that of another eigenvalue whose imaginary part eventually becomes larger than that of the former. Abdullah & Lindsay [1] are critical of the papers of Davey [7] and Fearn [12] in their analysis of higher Re values. According to linear theory for (1.2) and (1.3) the most unstable eigenvalue has largest imaginary part, i.e. c_i largest. Davey [7] claims the most unstable mode is symmetric, presumably on the basis that this is so for $Re = 10^4, a = 1$. Fearn [12] solves a symmetric problem and simply refers to *the solution* to (1.2), confirming Davey's [7] results. Abdullah & Lindsay [1] claim that these writers are using a tracking technique and miss the leading eigenvalue since mode crossing occurs. We have partially confirmed the findings of Abdullah & Lindsay [1] and Lindsay & Ogden [21] who only give the first five eigenvalues, although it would appear they find only symmetric ones. This is especially important, since for $Re = 10^5, a = 1$, we confirm mode crossing has occurred, but we find the leading eigenvalue to be skew-symmetric. We present in table 1 the leading eigenvalues for $Re = 10^5$ and $a = 1$, our calculations being made by a D^2 method, but determining odd modes and even modes separately, with $M = 200$ in each case, i.e. equivalent to $M = 400$ for the full problem.

Symmetry	Eigenvalue
A	$.9888191058E+00 - .1116257893E-01i$
A	$.9798738045E+00 - .2008374163E-01i$
A	$.9709280339E+00 - .2900433538E-01i$
A	$.1373944878E+00 - .2956356969E-01i$
A	$.9619817790E+00 - .3792441466E-01i$
A	$.9530350180E+00 - .4684401422E-01i$
S	$.9888195933E+00 - .1116360699E-01i$
S	$.1459247829E+00 - .1504203085E-01i$
S	$.9798751271E+00 - .2008635538E-01i$
S	$.9709305305E+00 - .2900898101E-01i$
S	$.1982003566E+00 - .3733100660E-01i$
S	$.9619857994E+00 - .3793148490E-01i$

Table 1. The six odd and six even eigenvalues with largest imaginary part for the Orr-Sommerfeld problem with $U = 1 - z^2$, $Re = 10^5$, $a = 1$. A=anti-symmetric, S=symmetric.

It is seen from table 1 that the "leading" eigenvalue is a skew - symmetric one. In table 2 we include components of the eigenvector for this skew mode; it is seen that machine precision is reached with 86 odd polynomials, i.e. up to T_{171}. (All components are not included, just a sample to demonstrate convergence.)

Com. No.	ϕ_r	ϕ_i	A_r	A_i
1	.208839E-03	.409542E-03	.240779E-01	.204308E-01
11	.421908E-03	.289300E-03	-.167597E+00	-.125165E+00
21	.889307E-04	-.897408E-04	-.147664E+00	.148864E+00
31	-.123273E-04	-.114027E-05	.458675E-01	.307459E-02
41	.461222E-06	.686801E-07	-.304143E-02	-.281158E-03
51	-.553081E-08	.346867E-08	.525270E-04	-.400853E-04
61	-.122030E-10	-.307889E-10	.231698E-06	.414265E-06
71	.456178E-13	-.465328E-13	-.665353E-09	.937961E-09
81	-.147851E-14	-.190889E-14	-.960477E-12	.301479E-12
86	.153318E-14	.354368E-14	-.262614E-14	.292893E-14

Table 2. Some of the components of the eigenvector corresponding to $\sigma^{(1)} = 0.9888191058 - 0.01116257893i$, $Re = 10^5$, $a = 1$. Com. No. refers to the component of the eigenvector, $\phi = \phi_r + i\phi_i$, $A = A_r + iA_i$.

We have used the separate "odd" and "even" codes with $M = 200$ to compute the eigenvalues in the transistion region. For $a = 1$, in table 3 it is seen that the structure at $Re = 10^4$ is maintained at $Re = 80,822$ but by $Re = 80,828$ the first two eigenvalues exchange positions, then by $Re = 80,830$ the eigenvalue which is second at $Re = 80,828$ exchanges with the one occupying third position for the same Re value. The position of these three is maintained in table 1.

Symmetry	Eigenvalue	Re
A	$.9875629891E+00-.1241421339E-01i$	80822
A	$.9776125822E+00-.2233449266E-01i$	80822
A	$.1470238117E+00-.3124631640E-01i$	80822
A	$9676615245E+00-.3225401228E-01i$	80822
S	$.1555554132E+00-.1241409956E-01i$	80822
S	$.9875636361E+00-.1241555934E-01i$	80822
S	$.9776143504E+00-.2233791980E-01i$	80822
S	$.9676648840E+00-.3226011142E-01i$	80822
A	$.9875634508E+00-.1241375347E-01i$	80828
A	$.9776134133E+00-.2233366562E-01i$	80828
A	$.1470203436E+00-.3124575284E-01i$	80828
A	$.9676627251E+00-.3225281822E-01i$	80828
S	$.1555521082E+00-.1241509695E-01i$	80828
S	$.9875640977E+00-.1241509935E-01i$	80828
S	$.9776151812E+00-.2233709233E-01i$	80828
S	$.9676660845E+00-.3225891687E-01i$	80828
A	$.9875636047E+00-.1241360017E-01i$	80830
A	$.9776136903E+00-.2233338998E-01i$	80830
A	$.1470191935E+00-.3124557862E-01i$	80830
A	$.9676631252E+00-.3225242025E-01i$	80830
S	$.9875642516E+00-.1241494596E-01i$	80830
S	$.1555510002E+00-.1241538251E-01i$	80830
S	$.9776154583E+00-.2233681675E-01i$	80830
S	$.9676664843E+00-.3225851880E-01i$	80830

Table 3. The four leading odd and even eigenvalues in the transistion region, $M = 200$, $a = 1$.

Abdullah & Lindsay [1] report further mode crossings for higher Re values. However, much care must be taken when Re increases. We now report findings for the spectrum and in particular in the region near the joining of the so called A, P and S branches -

the three groups of branches in figure 1. The A branches are the upper left ones, the P branch is the upper right one composed of degenerate pairs, and the S branch is the lower one emanating from $c_r = 2/3$; this notation is standard in the fluid dynamics literature, see Drazin & Reid [11], Mack [23]. The eigenvalues near the branch point are particularly sensitive to change, Orszag [27], and we find great care must be taken even with Re around 2.3×10^4.

We have computed many cases and figures 2-5 below are just a sample. Even though they are only for even modes they illustrate the important points regarding round off error; the same findings are true for odd mode cases, and for the full code which finds odd and even modes together.

Figures 2 to 5 are obtained with the D^2 method solving (1.2), (1.3) for even modes only, i.e. employing only even polynomials, using full precision arithmetic (64 bit) in figures 2 to 4, whereas extended precision (128 bit) is employed in figure 5. Figure 2 demonstrates inaccuracy caused by having insufficient polynomials, even though $M = 85$, (equivalent to 170 in the odd and even code); this splitting in the tail is symptomatic of insufficient polynomials and has been seen in pipe flow by Davey & Drazin [8] and Schmid & Henningson [32]. By increasing the number of polynomials we are able to overcome the splitting of the tail problem as in figure 3 where $M = 200$. Nevertheless, the eigenvalues at the intersection are not accurate. Increasing the number of polynomials compounds the problem and we find a "triangle of numerical instability" begins to form, figure 4, where $M = 500$. We have found that this behaviour is due to the precision to which we are working. By increasing from 64 to 128 bit arithmetic this effect is removed (in this case), see figure 5. We have not seen the latter effect reported before.

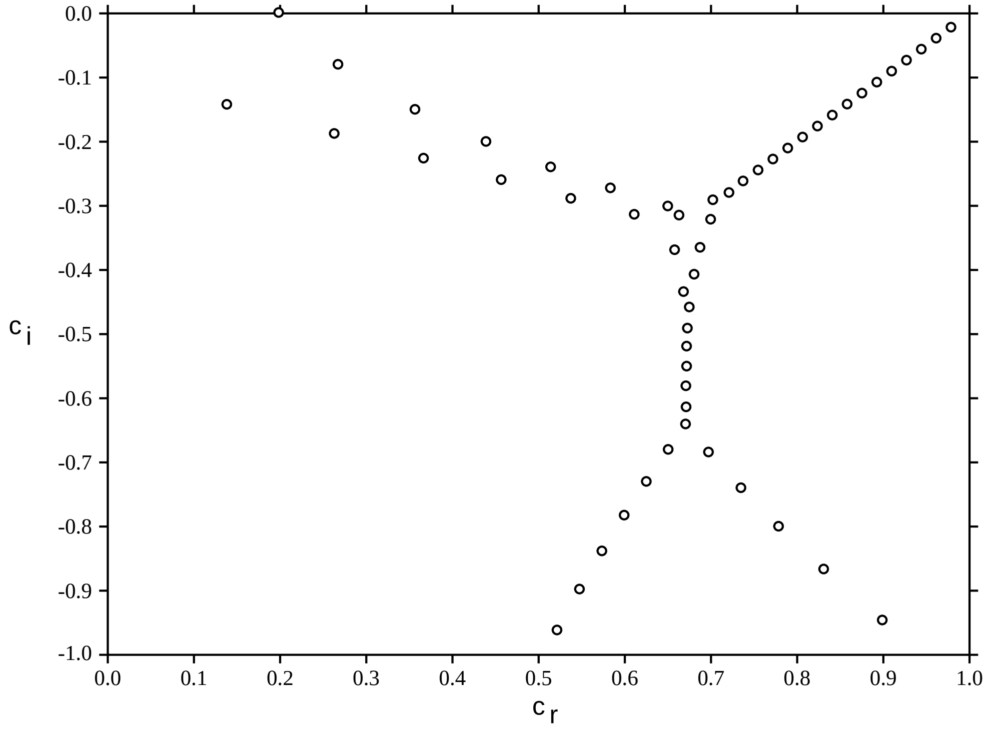

Figure 2 The even modes for plane Poiseuille flow. Effect of too few polynomials. $Re = 2.7 \times 10^4, a = 1, M = 85$, 64 bit arithmetic.

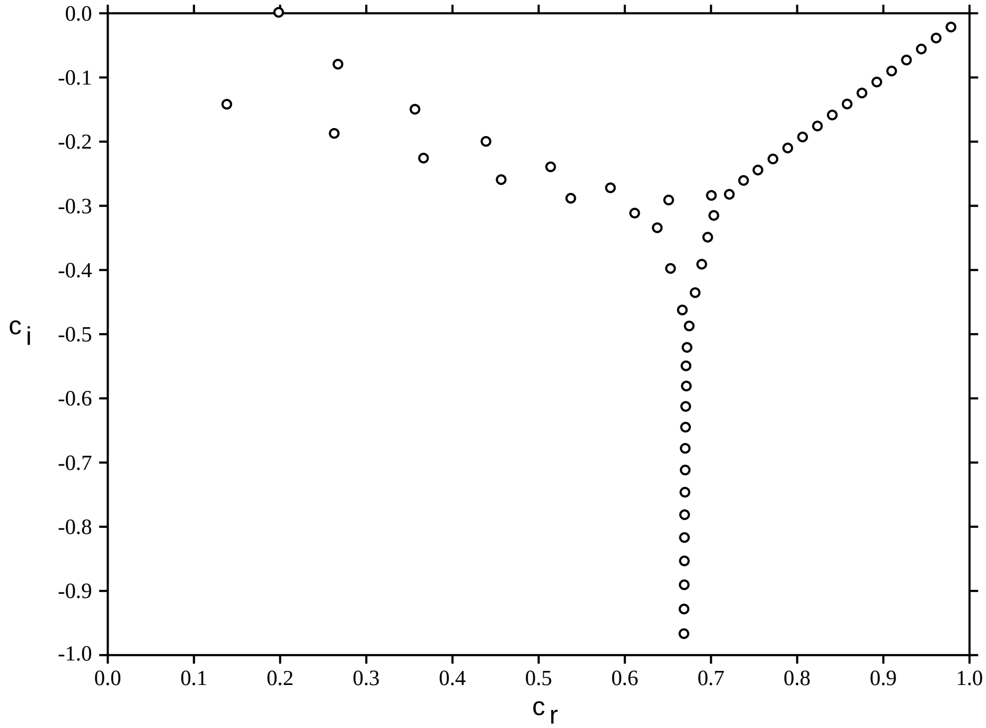

Figure 3 The even modes for plane Poiseuille flow. Effect of finite precision. $Re = 2.7 \times 10^4, a = 1, M = 200$, 64 bit arithmetic.

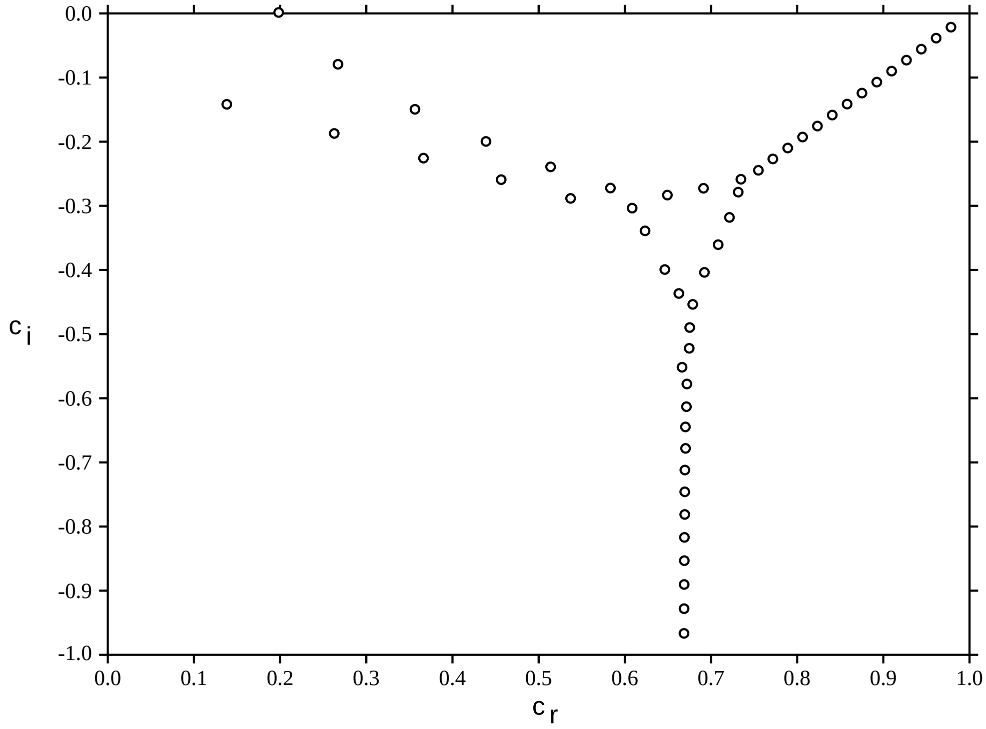

Figure 4 The even modes for plane Poiseuille flow. Effect of finite precision. $Re = 2.7 \times 10^4, a = 1, M = 500$, 64 bit arithmetic.

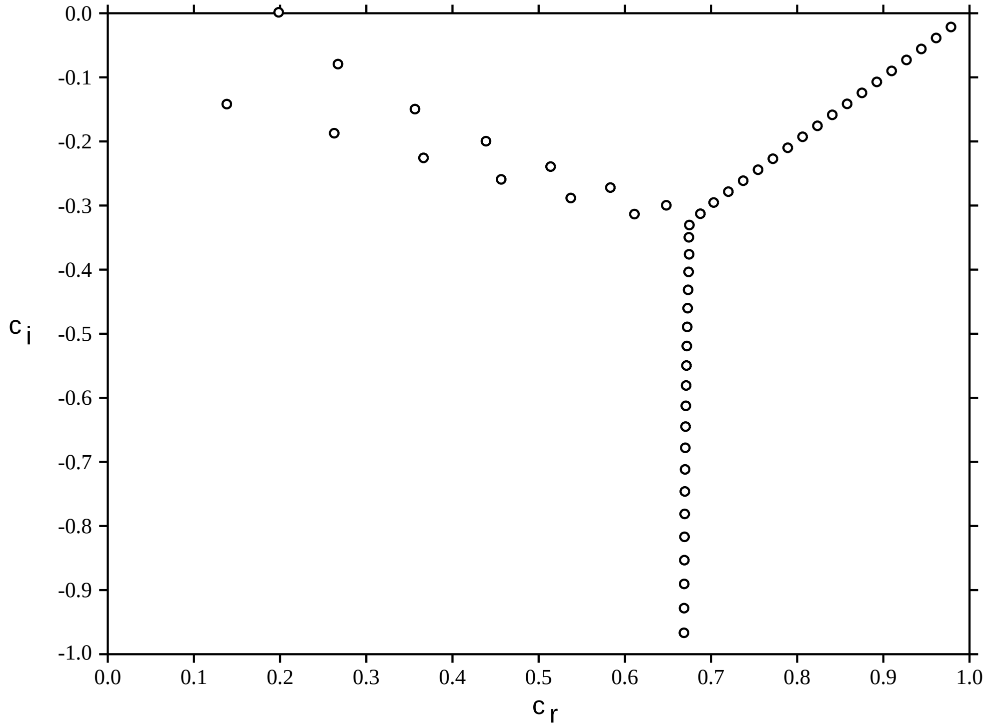

Figure 5 The even modes for plane Poiseuille flow. $Re = 2.7 \times 10^4, a = 1, M = 200$, 128 bit arithmetic.

Remarks. 1. We have drawn attention to three important types of error which are present in solving difficult eigenvalue problems. The first is round off error due to growth of matrix coefficients; in this respect a D^2 method is preferable to one using D^4. Secondly, too few polynomials causes the "tail", i.e. the S branch, to split. Thirdly, increasing the number of polynomials in a cavalier fashion to compute sensitive eigenvalues can lead to inaccuracy due to ill conditioning and insufficient precision in real number representation.

2. Pseudospectral methods may present an alternative for many of the calculations given here. They allow variable coefficient representation; however, so do the Chebyshev tau methods, and in our opinion, in a very easy manner. The accuracy obtained by Huang & Sloan [20], table IV p. 406, for the Orr-Sommerfeld problem with $Re = 10^4, a = 1$, is certainly no better than what we find with the D^2 and D methods. They do not detect spurious eigenvalues (for the problems treated there), but McFadden *et al.* [22] claim the stream function - vorticity method does not either; this we have verified for $Re = 10^4, a = 1$. Huang & Sloan [20] treat standard test problems in reasonable parameter ranges and do not apply their method to high Reynolds number flow for either the Couette or Poiseuille problems, or to the two fluid situation of section 6; these are more severe tests of a method.

3. The eigenvalue problem for plane Couette flow

The problem of this subsection is (1.2) and (1.3) when $U = z$. Physically it corresponds to the lower plate fixed while the upper plate is moved with constant velocity, generating a linear shear. This problem is always stable according to linear theory, cf. Rionero & Mulone [26]. Nevertheless, it is not a trivial eigenvalue problem from a numerical standpoint.

With 150 polynomials in the D^2 method we obtain excellent accuracy for $Re = 3000, a = 1$, in 64 bit arithmetic. Breakdown at the intersection of the branch points is evident around $Re = 3500$. However, the same code operating at 128 bit arithmetic yields an accurate spectrum. Figures 6 and 7 show this effect for $a = 1, Re = 3800$. There is agreement in the conjugate pairs in these figures, to at least 10 digits, even in full precision on the upper branches.

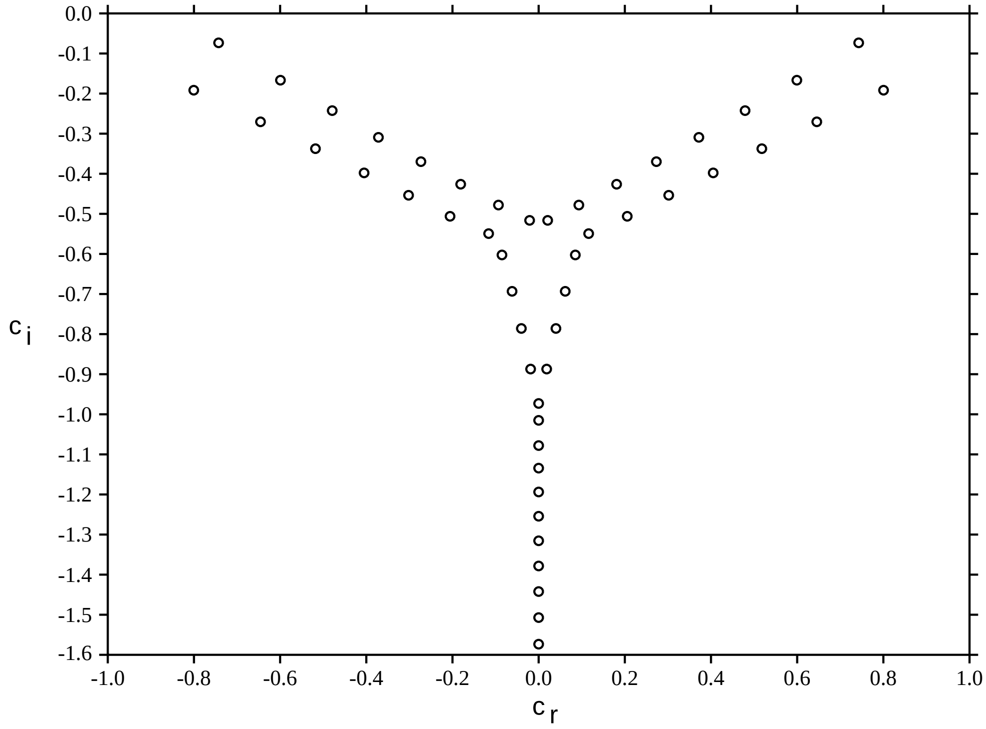

Figure 6 Numerical instability in the spectrum for plane Couette flow. $Re = 3800, a = 1, M = 150$, 64 bit arithmetic.

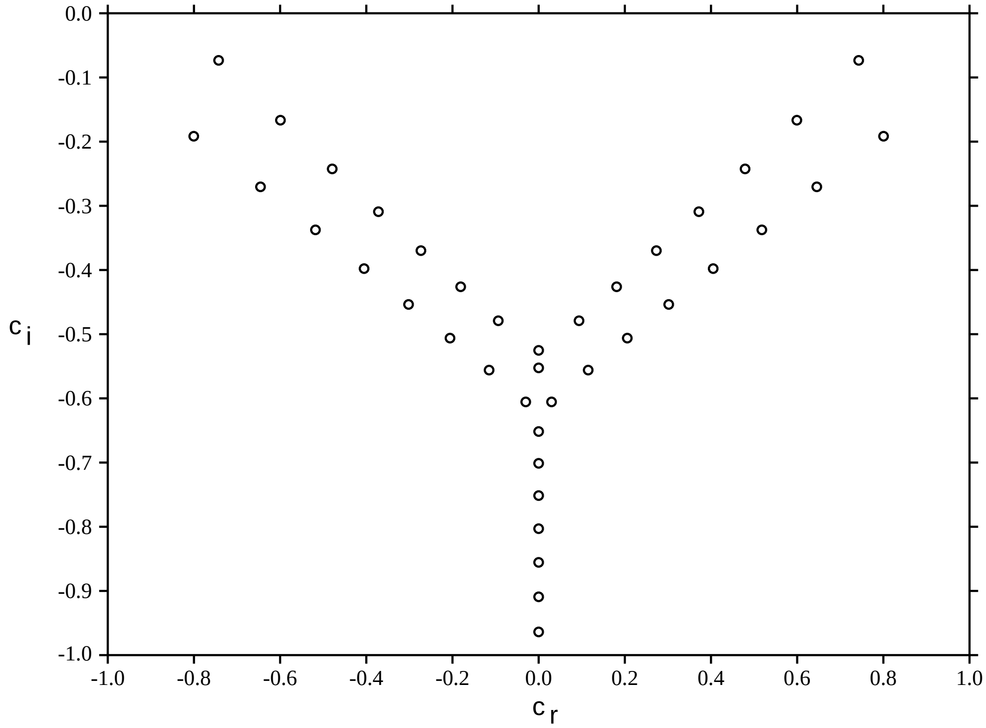

Figure 7 Effect of finite precision in the spectrum for plane Couette flow. $Re = 3800, a = 1, M = 150$, 128 bit arithmetic.

In 128 bit arithmetic we are able to extend the calculation well beyond $Re = 3800$. With 150 polynomials no difficulty is experienced at $Re = 8000$, but at $Re = 10^4$ a split in the tail is observed. By using 200 polynomials and 128 bit arithmetic we have been able to proceed to $Re = 13,000$, and the spectrum for this case is shown in figure 11, with actual numerical values tabulated in table 4.

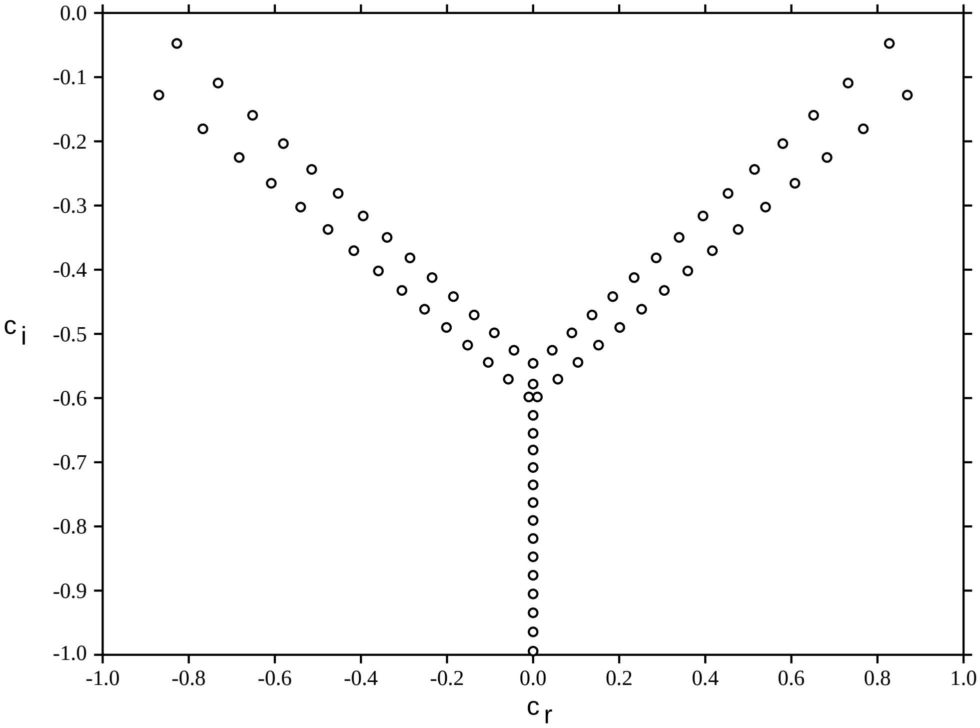

Figure 8 The spectrum for plane Couette flow, using 200 polynomials. $Re = 13,000, a = 1$, 128 bit arithmetic.

Mode number	Eigenvalue c
1	$\pm.8276152337E+00-.4751548439E-01i$
2	$\pm.7318167785E+00-.1091860424E+00i$
3	$\pm.8694486153E+00-.1279149536E+00i$
4	$\pm.6516804277E+00-.1594003003E+00i$
5	$\pm.7671186628E+00-.1805164930E+00i$
6	$\pm.5801567166E+00-.2035572830E+00i$
7	$\pm.6828371673E+00-.2251746419E+00i$
8	$\pm.5143995235E+00-.2437675825E+00i$
9	$\pm.6082408213E+00-.2653481107E+00i$
10	$\pm.4528935800E+00-.2811241939E+00i$
11	$\pm.5400219613E+00-.3024678732E+00i$
12	$\pm.3947096982E+00-.3162828159E+00i$
13	$\pm.4764491821E+00-.3373108149E+00i$
14	$\pm.3392256967E+00-.3496747907E+00i$
15	$\pm.4164746866E+00-.3703603829E+00i$
16	$\pm.2859989475E+00-.3816025000E+00i$
17	$\pm.3594042660E+00-.4019439818E+00i$
18	$\pm.2347002407E+00-.4122880439E+00i$
19	$\pm.3047483827E+00-.4322966352E+00i$
20	$\pm.1850762211E+00-.4419004929E+00i$
21	$\pm.2521456926E+00-.4615944208E+00i$
22	$\pm.1369265577E+00-.4705722463E+00i$
23	$\pm.2013199914E+00-.4899736516E+00i$
24	$\pm.9008929422E-01-.4984093248E+00i$
25	$\pm.1520542459E+00-.5175426311E+00i$
26	$\pm.4444142747E-01-.5255273887E+00i$
27	$\pm.1041741466E+00-.5443892453E+00i$
28	$.0000000000E+00-.5459244238E+00i$
29	$\pm.5753309952E-01-.5705930815E+00i$
30	$.0000000000E+00-.5782633202E+00i$
31	$\pm.9937461129E-02-.5982573646E+00i$
32	$.0000000000E+00-.6268958614E+00i$
33	$.0000000000E+00-.6550042769E+00i$
34	$.0000000000E+00-.6809093456E+00i$
35	$.0000000000E+00-.7081327166E+00i$
36	$.0000000000E+00-.7352566431E+00i$
37	$.0000000000E+00-.7628468874E+00i$
38	$.0000000000E+00-.7906653030E+00i$
39	$.0000000000E+00-.8188353645E+00i$
40	$.0000000000E+00-.8472841070E+00i$
41	$.0000000000E+00-.8760700653E+00i$
42	$.0000000000E+00-.9051510243E+00i$
43	$.0000000000E+00-.9345643207E+00i$
44	$.0000000000E+00-.9642865284E+00i$
45	$.0000000000E+00-.9943359829E+00i$

Table 4. The first 45 eigenvalues graphed in figure 11. Conjugate pairs are presented as one mode.

4. The eigenvalue problem for circular pipe flow

Symmetric disturbances for the linear instability problem for flow in a circular pipe driven by a constant pressure gradient (Hagen - Poiseuille flow) are governed by the equation

$$L^2\phi = iaRe(U-c)L\phi, \tag{4.1}$$

where a, Re, c are wavenumber, Reynolds number, and growth rate, respectively, the base velocity $U = 1 - r^2$, r being the radial coordinate, the differential operator L is defined by

$$L = \frac{d^2}{dr^2} - \frac{1}{r}\frac{d}{dr} - a^2, \tag{4.2}$$

and (4.1) holds on the domain $r \in (0,1)$. The disturbance ϕ is subject to the boundary conditions

$$\phi = \phi' = 0, \qquad r = 0, 1, \tag{4.3}$$

cf. Davey & Drazin [8], Drazin & Reid [11]. Symmetric disturbances governed by (4.1)-(4.3) are believed always stable, Davey & Drazin [8].

The boundary value problem (4.1)-(4.3) is easily solved by a D^2 method by writing

$$\begin{aligned} L\phi &= \psi, \\ L\psi &= iaRe(U-c)\psi, \end{aligned} \tag{4.4}$$

subject to (4.3). To use the Chebyshev tau method on this system we transform to $z = 2r - 1$ and then use the relation, Orszag [27],

$$T_{m+1}(z) + T_{m-1}(z) = 2zT_m(z), \quad m \geq 1. \tag{4.5}$$

System (4.4) is discretized by multiplying each equation by $(z+1)T_m$, to remove the singularity, and integrating in the weighted $L^2(-1,1)$ space with weight $(1-z^2)^{-1/2}$.

After employing (4.5) we arrive at an equation of form (1.1) where

$$A_r = \begin{pmatrix} 4ZD^2 + 4D^2 - 4D - a^2(Z+I) & -(Z+I) \\ BC1 & 0\dots0 \\ BC2 & 0\dots0 \\ & \\ 0 & 4ZD^2 + 4D^2 - 4D - a^2(Z+I) \\ BC3 & 0\dots0 \\ BC4 & 0\dots0 \end{pmatrix}$$

$$A_i = \begin{pmatrix} 0 & 0 \\ 0\dots0 & 0\dots0 \\ 0\dots0 & 0\dots0 \\ & \\ 0 & aRe(\frac{1}{4}Z^3 + \frac{3}{4}Z^2 - \frac{1}{4}Z - \frac{3}{4}I) \\ 0\dots0 & 0\dots0 \\ 0\dots0 & 0\dots0 \end{pmatrix}$$

and

$$B_r = \mathbf{0}, \qquad B_i = \begin{pmatrix} 0 & 0 \\ 0 & -aReI \\ & 0\ldots0 \\ & 0\ldots0 \end{pmatrix}$$

where

$$\mathbf{x} = (\phi_0, \ldots, \phi_N, \psi_0, \ldots, \psi_N)^T,$$

Z^n denotes the matrix arising from the Chebyshev representation of the function z^n, ZD^2 being the Chebyshev representation of zD^2. The boundary conditions $BC1 - BC4$ are a symmetric form of (4.3).

The figures below were all obtained in full precision arithmetic (64 bits). Figure 9 is the analogue of figure 1. Figure 10 shows the "splitting" of the spectrum due to insufficient polynomials, this having been seen previously by Davey & Drazin [8] and Schmid & Henningson [32]. Figure 11 shows the correct spectrum for the parameters of figure 10, and finally figures 12, 13 demonstrate what happens if too many polynomials are present without sufficient precision in the arithmetic.

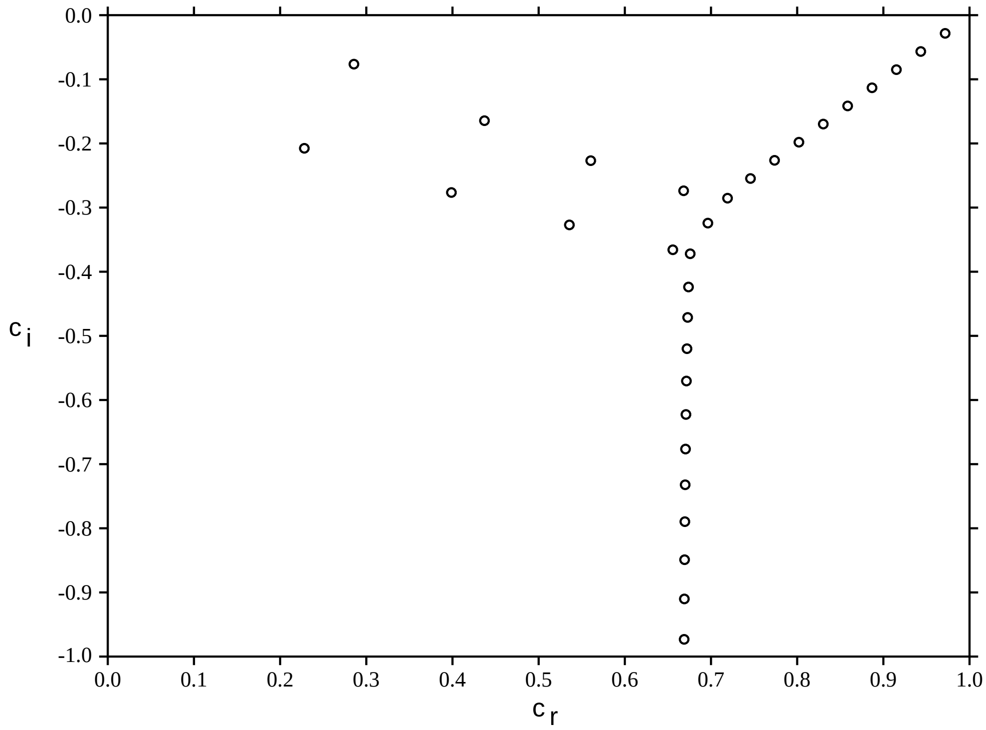

Figure 9 The spectrum for symmetric disturbances in Hagen - Poiseuille flow. $Re = 10^4, a = 1, M = 100$.

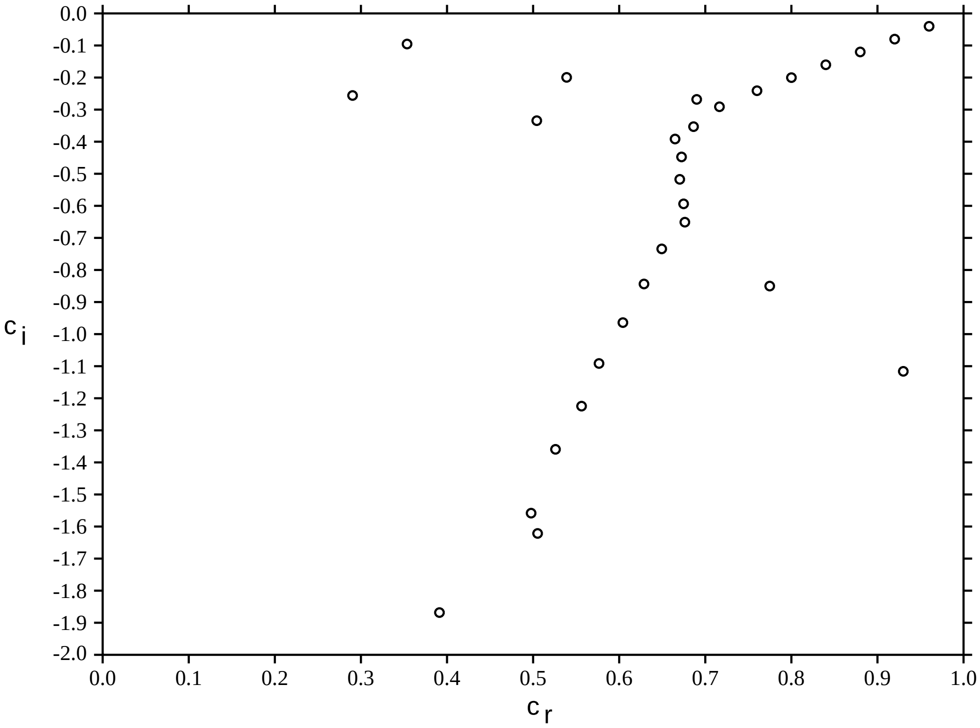

Figure 10 Effect of too few polynomials on the spectrum for symmetric disturbances in Hagen - Poiseuille flow. $Re = 5000, a = 1, M = 50$.

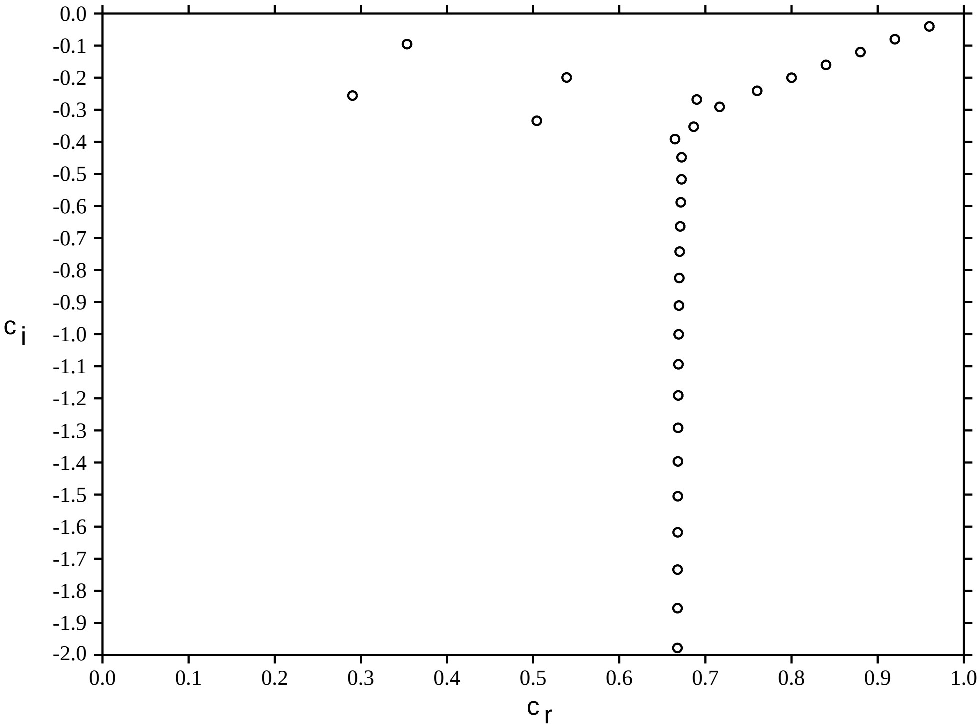

Figure 11 The spectrum for symmetric disturbances in Hagen - Poiseuille flow. $Re = 5000, a = 1, M = 100$.

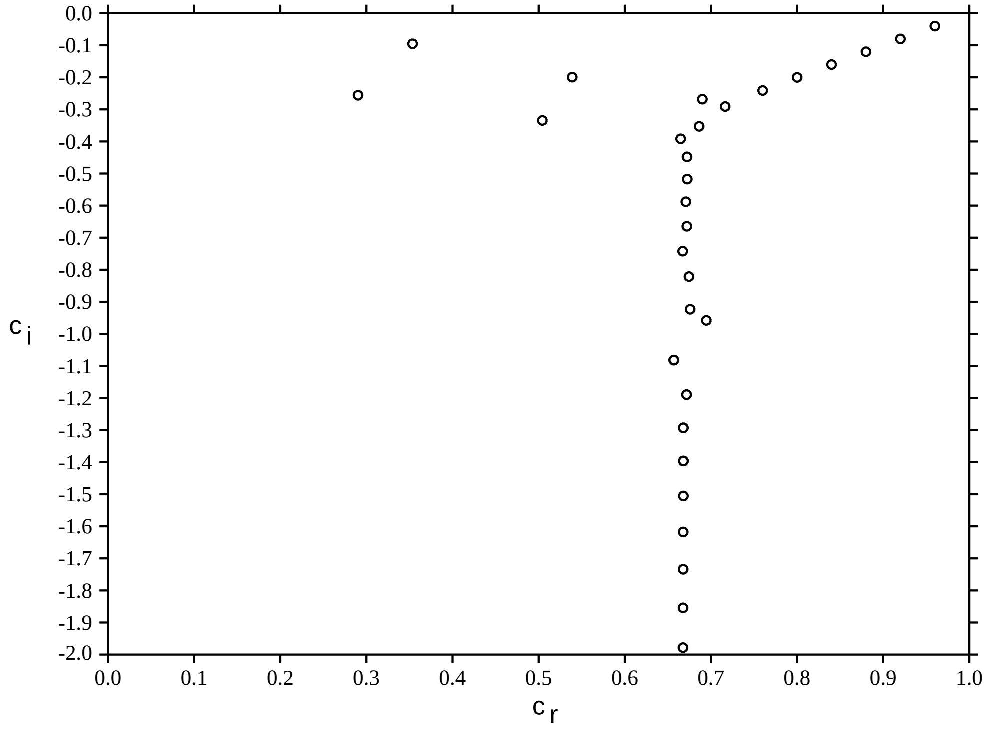

Figure 12 Effect of lack of precision and round off error on the spectrum for symmetric disturbances in Hagen - Poiseuille flow. $Re = 5000, a = 1, M = 250$.

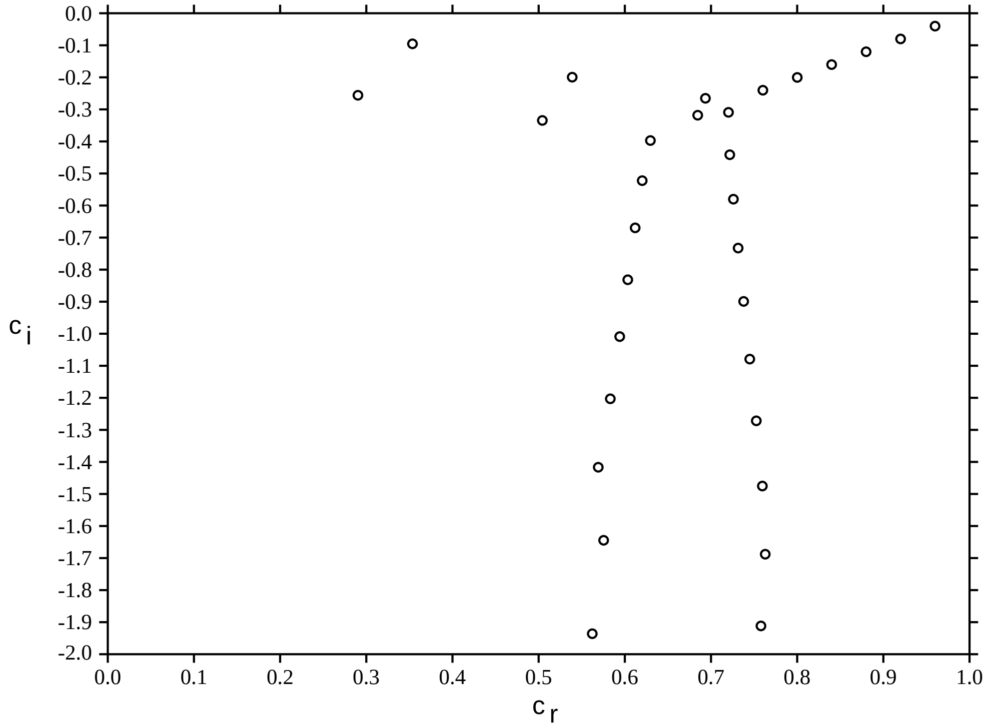

Figure 13 Effect of lack of precision and round off error on the spectrum for symmetric disturbances in Hagen - Poiseuille flow. $Re = 5000, a = 1, M = 400$.

5. Normal velocity - normal vorticity interactions

Butler & Farrell [3] is a very interesting paper studying transient growth between the component of normal velocity v and the component of normal vorticity $\omega = u_{,z} - w_{,x}$, i.e. in the y-direction; observe that this is not the vorticity in the stream function - vorticity method which would be $\omega_3 = v_{,x} - u_{,y}$. Note that we are following the convention of [3] that flow is in the x-direction and the plates are at $y = \pm 1$; this avoids confusion in w and ω later. Butler & Farrell [3] argue that the search for transient growth perturbations can be rationalised by determining the initial conditions which gain the most energy over a chosen time period. The technique they employ to find three-dimensional disturbances over a certain time interval is a variational one based on the kinetic energy. They point out that the differential equations describing shear like flows in a viscous fluid are not self-adjoint in the spaces of physical interest and thus a perturbation may consist of modes which initially destructively interfere, after which they separate in time revealing considerable growth in the mean kinetic energy of the perturbation. The local growth analysis of [3] is based on the eigenvalue problem for interaction of the normal velocity, v, and normal vorticity, ω. This eigenvalue problem is

$$\begin{aligned}\Delta^2 v - iaReU\Delta v + iaReU''v &= Re\,\sigma\Delta v,\\ \Delta\omega - iaReU\omega - ibReU'v &= Re\,\sigma\omega,\end{aligned}\tag{5.1}$$

where $U = y$, for Couette flow, $U = 1 - y^2$, for Poiseuille flow, a and b are the x and z wave numbers and Δ is the three-dimensional Laplacian. The growth rate here is σ; we do make a comparison with the growth rate as defined in earlier sections which may be formally taken as $\sigma = -iac$, although this is only suggestive due to the presence of b. The functions v, ω satisfy the boundary conditions

$$v = \frac{\partial v}{\partial y} = \omega = 0, \qquad y = \pm 1. \tag{5.2}$$

In their numerical calculations Butler & Farrell [3] employ a finite difference method together with the QR algorithm for finding the eigenvalues.

In this paper we only treat Poiseuille flow so henceforth $U = 1 - y^2$. To solve (5.1), (5.2) by a D^2 Chebyshev tau - QZ algorithm method we write (5.1) as a system of three second order equations

$$\begin{aligned}&(D^2 - k^2)v - \chi = 0,\\ &(D^2 - k^2)\chi - iaReU\chi - 2iaRe\,v = Re\,\sigma\chi,\\ &(D^2 - k^2)\omega - iaReU\omega + 2ibyRe\,v = Re\,\sigma\omega,\end{aligned}\tag{5.3}$$

where $k^2 = a^2 + b^2$ and $D = d/dy$. These equations are discretized by writing v, χ, ω as a series in $N + 1$ Chebyshev polynomials and taking inner products with T_m to yield an equation of form (1.1) where A and B are $3M \times 3M$ complex matrices with B singular, given by

$$A_r = \begin{pmatrix} D^2 - k^2 I & -I & 0 \\ BC1 & 0\dots0 & 0\dots0 \\ BC2 & 0\dots0 & 0\dots0 \\[1ex] 0 & D^2 - k^2 I & 0 \\ BC3 & 0\dots0 & 0\dots0 \\ BC4 & 0\dots0 & 0\dots0 \\[1ex] 0 & 0 & D^2 - k^2 I \\ 0\dots0 & 0\dots0 & BC5 \\ 0\dots0 & 0\dots0 & BC6 \end{pmatrix}$$

$$A_i = \begin{pmatrix} 0 & 0 & 0 \\[1ex] -2aReI & -aReU & 0 \\ 0\dots0 & 0\dots0 & 0\dots0 \\ 0\dots0 & 0\dots0 & 0\dots0 \\[1ex] 2bReY & 0 & -aReU \\ 0\dots0 & 0\dots0 & 0\dots0 \\ 0\dots0 & 0\dots0 & 0\dots0 \end{pmatrix}$$

and

$$B_i = \mathbf{0}, \qquad B_r = \begin{pmatrix} 0 & 0 & 0 \\[1ex] 0 & ReI & 0 \\ 0\dots0 & 0\dots0 & 0\dots0 \\ 0\dots0 & 0\dots0 & 0\dots0 \\[1ex] 0 & 0 & ReI \\ 0\dots0 & 0\dots0 & 0\dots0 \\ 0\dots0 & 0\dots0 & 0\dots0 \end{pmatrix}$$

where $U = I - Y^2$ is the matrix representation of $U(y)$ arising from the Chebyshev representation of y, and

$$\mathbf{x} = (v_0, \dots, v_N, \chi_0, \dots, \chi_N, \omega_0, \dots, \omega_N)^T.$$

The boundary condition rows $BC1 - BC6$ are simply the discrete versions of (5.2), which we write in a symmetric way.

In the formal limit $b \to 0$ the first two equations of (5.3) reduce to the standard Orr-Sommerfeld equation for plane Poiseuille flow while the third equation in (5.3) gives Squire modes, [3]. We include some output from solving our (1.1) version of (5.3). In the figures below we graph $c = i\sigma/a$ to obtain a direct comparison with the usual formulation of plane Poiseuille flow as in section 2. Figure 14 shows the spectrum for $Re = 5000, a = 1, b = 0$. The Orr-Sommerfeld modes are seen together with the Squire modes. Figures 15, 16 show the effect of increasing the coupling term b; interestingly the eigenvalue which is dominant in two-dimensional flow theory rapidly decreases (in imaginary part) with increasing b. Figure 17 includes a plot of "the spectrum" for a case in some sense close to Butler & Farrell's [3] optimal situation of $a = 0, b = 2.044$ for $Re = 5000$; the spectrum is seen to be much changed.

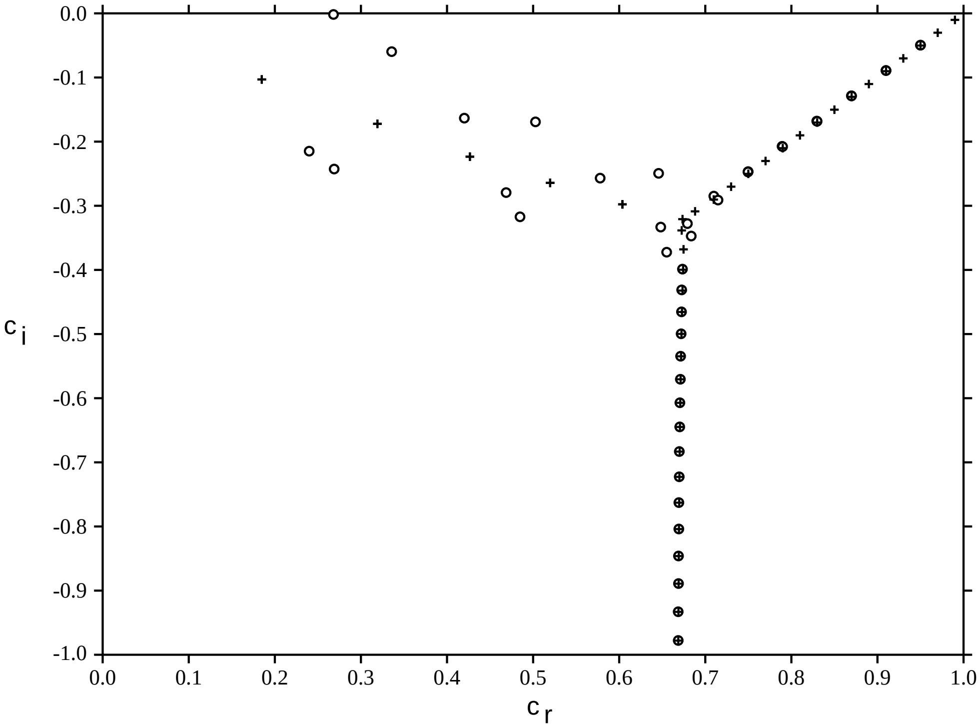

Figure 14 The spectrum for (5.3). $Re = 5000, a = 1, b = 0$. Open circle (o) = Orr-Sommerfeld mode, cross (+) = Squire mode.

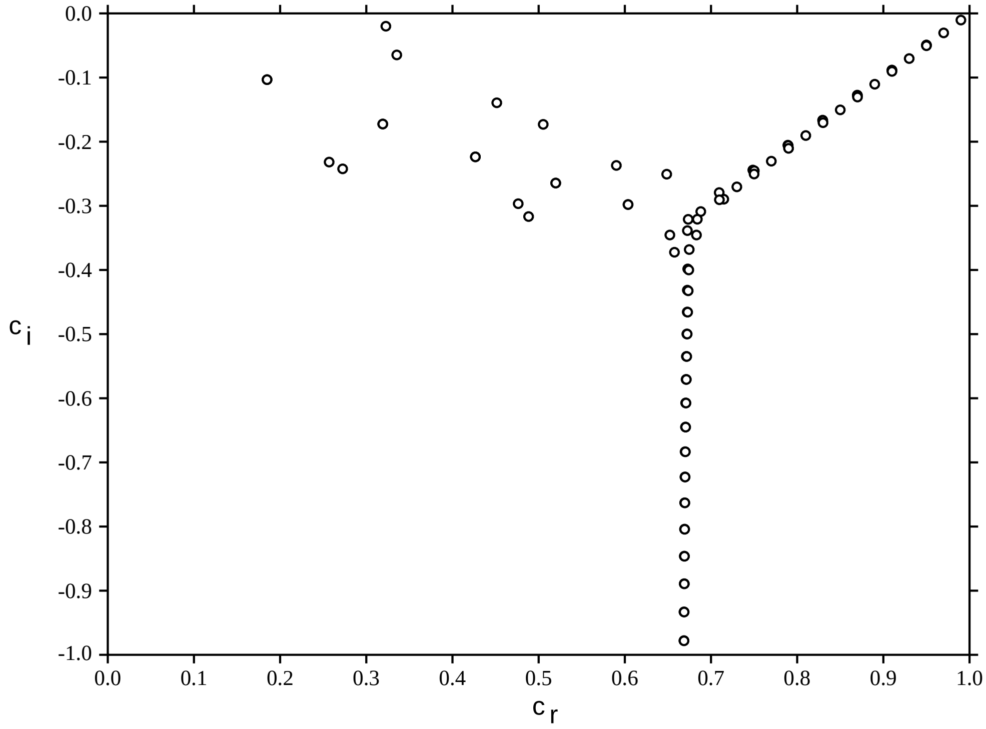

Figure 15 The spectrum for (5.3). $Re = 5000, a = 1, b = 1$.

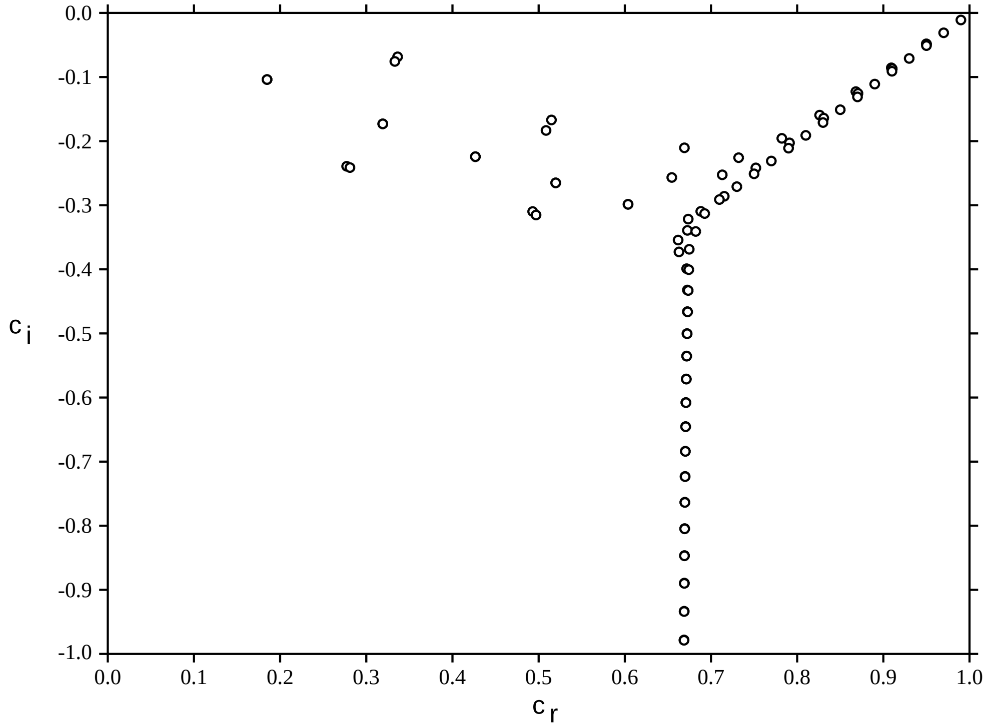

Figure 16 The spectrum for (5.3). $Re = 5000, a = 1, b = 2$.

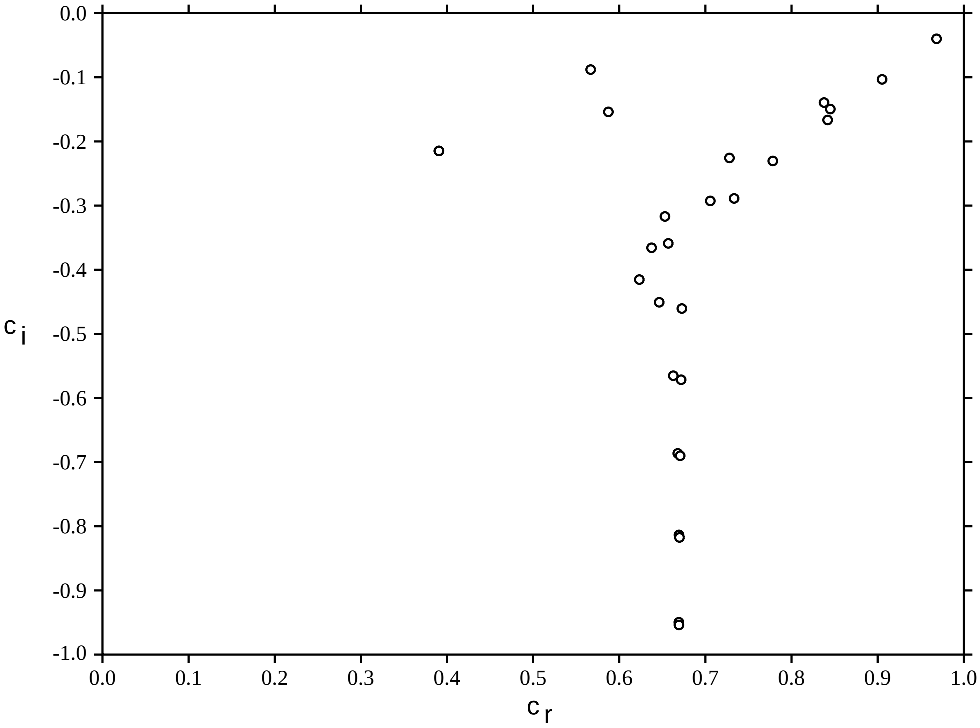

Figure 17 The spectrum for (5.3). $Re = 5000, a = 0.1, b = 2.044$.

6. The eigenvalue problem for Orr-Sommerfeld like flows for two superposed immiscible fluids.

Here we study the eigenvalue problem associated to the problem of Couette and / or Poiseuille flow when one immiscible viscous fluid overlies another. This is a problem of major technological importance with application from the oil industry to fields such as de-icing of an aeroplane wing, cf. Chen & Crighton [5]; many references may be found in the papers by Chen & Crighton [5], Hooper [19], and Renardy [30]. While we here develop a D^2 method for the situation studied by Hooper [19] we believe the ideas are extendable to more complicated scenarios such as the one of Chen & Crighton [5].

Hooper [19] assumes a fluid, denoted by 2, is overlying a different, immiscible fluid, denoted by 1, the configuration being contained in a horizontal position between planes $y = -1, y = n$, with the $(x, z)-$plane horizontal while the $y-$axis is vertical (orthogonal to the bounding planes of the fluids). The dynamic viscosities, densities and depths in each fluid are denoted by μ_α, ρ_α and d_α, respectively, $\alpha = 1, 2$. The upper plane $y = n$ may be subject to a (dimensionless) velocity in the $x-$direction, u_n, and the velocity of the interface (in the steady state) is $U_{\rm int}$. A Reynolds number, R, is defined with respect to U_{int}. The basic flow has form

$$\begin{aligned} u_1(y) =& A_1y^2 + a_1y + 1, \qquad -1 < y < 0, \\ u_2(y) =& A_2y^2 + a_2y + 1, \qquad 0 < y < n, \end{aligned} \tag{6.1}$$

where

$$\begin{aligned} A_1 &= \frac{-(m+n) + mu_n}{n(n+1)}, \\ a_1 &= \frac{n^2 - m + mu_n}{n(n+1)}, \\ A_2 &= \frac{A_1}{m}, \qquad a_2 = \frac{a_1}{m}, \end{aligned} \tag{6.2}$$

with m and n being the viscosity and depth ratios,

$$m = \frac{\mu_2}{\mu_1}, \qquad n = \frac{d_2}{d_1}. \tag{6.3}$$

Hooper [19] observes that $u_n = 0$ gives rise to a two fluid version of plane Poiseuille flow, whereas $u_n = (m+n)/m$ yields Couette flow. Renardy [30], pp. 1762, 1763, includes a detailed account of the applicability of Squire's theorem to two fluid flows and points out that if there are islands of stability (where the neutral curve consists of one or more isolated closed curves in addition to the usual convex one, as occurs in multi - component convection - diffusion, cf. Straughan & Walker [37]) then such a theorem would not be applicable. In that case one would be faced with a three-dimensional analysis and a D^2 method is not equivalent to a stream function - vorticity method. We here follow Hooper [19] and analyse directly the two-dimensional situation. Hooper [19] shows the effective stream function ϕ_α in each fluid satisfies the equations

$$\begin{aligned} \left(\frac{d^2}{dy^2} - a^2\right)^2 \phi_1(y) =& i\alpha R\Big\{ \big[u_1(y) - c\big]\left(\frac{d^2}{dy^2} - a^2\right) \\ & - u_1''(y)\Big\}\phi_1(y), \qquad -1 < y < 0, \end{aligned} \tag{6.4}$$

$$\begin{aligned} \left(\frac{d^2}{dy^2} - a^2\right)^2 \phi_2(y) =& \frac{i\alpha R}{m}\Big\{ \big[u_2(y) - c\big]\left(\frac{d^2}{dy^2} - a^2\right) \\ & - u_2''(y)\Big\}\phi_2(y), \qquad 0 < y < n, \end{aligned} \tag{6.5}$$

where a is the wavenumber and c is the growth rate due to a disturbance of form $\exp[ia(x-ct)]$.

The boundary conditions on the plates are

$$\phi_1(-1) = 0, \quad \phi_1'(-1) = 0, \qquad \phi_2(n) = 0, \quad \phi_2'(n) = 0. \tag{6.6}$$

The interface conditions due to continuity of velocity components and continuity of shear and normal stresses are, on $y = 0$,

$$\begin{aligned}
&\phi_1 = \phi_2 \quad (= \phi(0)),\\
&\phi_1' = \phi_2' + \frac{\phi(0)}{[c - u_1(0)]}\, u_1'(0)\Big(\frac{1-m}{m}\Big),\\
&\phi_1'' + a^2\phi_1 = m(\phi_2'' + a^2\phi_2),\\
&-iaR\big([c - u_1(0)]\phi_1' + a_1\phi_1\big) + iraR\big([c - u_1(0)]\phi_2' + a_2\phi_2\big)\\
&\qquad -\phi_1''' + 3a^2\phi_1' + m(\phi_2''' - 3a^2\phi_2') = \frac{iaR}{[c - u_1(0)]}\left(\frac{1}{F^2} + a^2 S\right)\phi,
\end{aligned} \tag{6.7}$$

where $r = \rho_1/\rho_2$, F is a non-dimensional form of the density difference $\rho_2 - \rho_1$, and S is a non-dimensional form of the interfacial tension, Yih [39]. Actually, Hooper [19] restricts attention to equal densities and zero interfacial tension, i.e. $r = 1, S = 0$, as we do in computations. However, we wish to indicate that the D^2 method may be applied to the complete boundary condition due to continuity of normal stress, $(6.7)_4$, derived by Yih [39].

To implement $(6.7)_4$ in practice we use $(6.7)_2$ to rewrite it as

$$\begin{aligned}
&-iaR\big([c - u_1(0)]\phi_1' + a_1\phi_1\big) + iraR\big([c - u_1(0)]\phi_2' + a_2\phi_2\big)\\
&\qquad -\phi_1''' + 3a^2\phi_1' + m(\phi_2''' - 3a^2\phi_2') = \frac{iaRm}{u_1'(0)(1-m)}\left(\frac{1}{F^2} + a^2 S\right)(\phi_1' - \phi_2'),
\end{aligned} \tag{6.8}$$

with $m \neq 1$. A discrete version of (6.8) is easily added to a Chebyshev formulation, following the lines given below.

Henceforth, we restrict attention to Hooper's [19] problem for which $r = 1, S = 0$. To solve (6.4)-(6.7) by a D^2 Chebyshev tau - QZ algorithm technique we first map $y \in (-1, 0)$ and $y \in (0, n)$ to the domains $(-1, 1)$ by the transformations

$$z_1 = -2y - 1, \quad z_2 = \frac{2}{n}\,y - 1; \tag{6.9}$$

note that $z = -1$ becomes the interface in both cases.

Define now $\phi(z_1) = \phi_1(y), \psi(z_2) = \phi_2(y)$, and then define the differential operators

L_1, L_2, and functions ξ, ω by

$$\begin{aligned} L_1\phi &\equiv \Big(4\frac{d^2}{dz_1^2} - a^2\Big)\phi, \\ L_1\phi &= \xi, \\ L_2\psi &\equiv \Big(\frac{4}{n^2}\frac{d^2}{dz_2^2} - a^2\Big)\psi, \\ L_2\psi &= \omega, \end{aligned} \tag{6.10}$$

so we rewrite the differential equations (6.4), (6.5) as

$$\begin{aligned} &L_1\phi - \xi = 0, \\ &L_1\xi - iaRu_1\xi + 2A_1 iaR\phi = -ciaR\xi, \\ &L_2\psi - \omega = 0, \\ &L_2\omega - i\frac{aR}{m}u_2\omega + 2A_2 i\frac{aR}{m}\psi = -ci\frac{aR}{m}\omega. \end{aligned} \tag{6.11}$$

The idea is to write

$$\phi = \sum_{n=0}^{N+2}\phi_n T_n(z_1), \quad \xi = \sum_{n=0}^{N+2}\xi_n T_n(z_1), \quad \psi = \sum_{n=0}^{N+2}\psi_n T_n(z_2), \quad \omega = \sum_{n=0}^{N+2}\omega_n T_n(z_2).$$

The boundary conditions (6.6) become

$$\phi(1) = \frac{d\phi}{dz_1}(1) = 0, \qquad \psi(1) = \frac{d\psi}{dz_2}(1) = 0. \tag{6.12}$$

The interface boundary conditions are, on $z_1 = z_2 = -1$,

$$\begin{aligned} &\phi - \psi = 0, \\ &\xi + 2a^2\phi - m\omega - 2a^2 m\psi = 0, \\ &\frac{d\xi}{dz_1} - 2a^2\frac{d\phi}{dz_1} + \frac{m}{n}\frac{d\omega}{dz_2} - \frac{2m}{n}a^2\frac{d\psi}{dz_2} = 0, \\ &c\Big(\frac{d\phi}{dz_1} + \frac{1}{n}\frac{d\psi}{dz_2}\Big) = \frac{d\phi}{dz_1} + \frac{1}{n}\frac{d\psi}{dz_2} - \frac{a_1}{2}\Big(\frac{1-m}{m}\Big)\phi. \end{aligned} \tag{6.13}$$

The Chebyshev tau version of (6.11)-(6.13) yields a $4(N+3) \times 4(N+3)$ matrix system like (1.1) where

$$A_r = \begin{pmatrix}
4D^2 - a^2 I & -I & 0 & 0 \\
BC1 & 0\dots 0 & 0\dots 0 & 0\dots 0 \\
BC2 & 0\dots 0 & 0\dots 0 & 0\dots 0 \\[1em]
0 & 4D^2 - a^2 I & 0 & 0 \\
BC5 & BC5 & BC5 & BC5 \\
BC6 & BC6 & BC6 & BC6 \\[1em]
0 & 0 & \frac{4}{n^2}D^2 - a^2 I & 0 \\
0\dots 0 & 0\dots 0 & BC3 & 0\dots 0 \\
0\dots 0 & 0\dots 0 & BC4 & 0\dots 0 \\[1em]
0 & 0 & 0 & \frac{4}{n^2}D^2 - a^2 I \\
BC7 & BC7 & BC7 & BC7 \\
BC8 & BC8 & BC8 & BC8
\end{pmatrix}$$

$$A_i = \begin{pmatrix}
0 & 0 & 0 & 0 \\
0\dots 0 & 0\dots 0 & 0\dots 0 & 0\dots 0 \\
0\dots 0 & 0\dots 0 & 0\dots 0 & 0\dots 0 \\[1em]
2aA_1RI & -aRu_1 & 0 & 0 \\
0\dots 0 & 0\dots 0 & 0\dots 0 & 0\dots 0 \\
0\dots 0 & 0\dots 0 & 0\dots 0 & 0\dots 0 \\[1em]
0 & 0 & 0 & 0 \\
0\dots 0 & 0\dots 0 & 0\dots 0 & 0\dots 0 \\
0\dots 0 & 0\dots 0 & 0\dots 0 & 0\dots 0 \\[1em]
0 & 0 & 2\frac{A_2 aR}{m} I & -\frac{aR}{m} u_2 \\
0\dots 0 & 0\dots 0 & 0\dots 0 & 0\dots 0 \\
0\dots 0 & 0\dots 0 & 0\dots 0 & 0\dots 0
\end{pmatrix}$$

$$B_r = \begin{pmatrix}
0 & 0 & 0 & 0 \\
0\dots 0 & 0\dots 0 & 0\dots 0 & 0\dots 0 \\
0\dots 0 & 0\dots 0 & 0\dots 0 & 0\dots 0 \\[1em]
0 & 0 & 0 & 0 \\
0\dots 0 & 0\dots 0 & 0\dots 0 & 0\dots 0 \\
0\dots 0 & 0\dots 0 & 0\dots 0 & 0\dots 0 \\[1em]
0 & 0 & 0 & 0 \\
0\dots 0 & 0\dots 0 & 0\dots 0 & 0\dots 0 \\
0\dots 0 & 0\dots 0 & 0\dots 0 & 0\dots 0 \\[1em]
0 & 0 & 0 & 0 \\
0\dots 0 & 0\dots 0 & 0\dots 0 & 0\dots 0 \\
BC8 & BC8 & BC8 & BC8
\end{pmatrix}$$

and

$$B_i = \begin{pmatrix} 0 & 0 & 0 & 0 \\ 0\ldots0 & 0\ldots0 & 0\ldots0 & 0\ldots0 \\ 0\ldots0 & 0\ldots0 & 0\ldots0 & 0\ldots0 \\[1ex] 0 & -aRI & 0 & 0 \\ 0\ldots0 & 0\ldots0 & 0\ldots0 & 0\ldots0 \\ 0\ldots0 & 0\ldots0 & 0\ldots0 & 0\ldots0 \\[1ex] 0 & 0 & 0 & 0 \\ 0\ldots0 & 0\ldots0 & 0\ldots0 & 0\ldots0 \\ 0\ldots0 & 0\ldots0 & 0\ldots0 & 0\ldots0 \\[1ex] 0 & 0 & 0 & -\frac{aR}{m}I \\ 0\ldots0 & 0\ldots0 & 0\ldots0 & 0\ldots0 \\ 0\ldots0 & 0\ldots0 & 0\ldots0 & 0\ldots0 \end{pmatrix}$$

where u_1 and u_2 are the Chebyshev representations of $u_1(z_1)$, $u_2(z_2)$, and

$$\mathbf{x} = (\phi_0, \ldots, \phi_N, \xi_0, \ldots, \xi_N, \psi_0, \ldots, \psi_N, \omega_0, \ldots, \omega_N)^T.$$

Let us assume N is rescaled so that each block is $N \times N$, i.e. each matrix is $4N \times 4N$. The BC1 terms, in row $N-1$, stand for the Chebyshev version of the boundary conditions $\phi(1) = 0$, and the BC2 terms, in row N, mean the boundary condition $\phi'(1) = 0$; these are written with the aid of the properties $T_n(\pm1) = (\pm1)^n$, $\quad T'_n(\pm1) = (\pm1)^{n-1}n^2$, Orszag [27]. Likewise the BC3 and BC4 terms, in rows $3N-1$ and $3N$, respectively, overwrite with the boundary conditions $\psi(1) = 0$ and $\psi'(1) = 0$. The BC5 - BC8 rows stand for the interface boundary conditions (6.13). The expression BC5 overwrites with

$$\phi(-1) \qquad 0 \qquad -\psi(-1) \qquad 0$$

i.e.

$$1 - 1 \ldots 1 - 1 \qquad 0\ldots0 \qquad -1\ 1 \ldots -1\ 1 \qquad 0\ldots0$$

where each group, e.g. $1 - 1 \ldots 1 - 1$, etc., contains N terms. The expression BC6 stands for

$$2a^2\phi(-1) \qquad \xi(-1) \qquad -2a^2 m\psi(-1) \qquad -m\omega(-1)$$

while the notation BC7 overwrites with

$$-2a^2\frac{d\phi}{dz_1}(-1) \qquad \frac{d\xi}{dz_1}(-1) \qquad -2\frac{m}{n}a^2\frac{d\psi}{dz_2}(-1) \qquad \frac{m}{n}\frac{d\omega}{dz_2}(-1).$$

The interface boundary condition $(6.13)_4$ involving c has to be written into row $4N$ of A_r and B_r, via BC8; the part going into A_r is

$$\frac{d\phi}{dz_1}(-1) - \frac{1}{2}a_1\Big(\frac{1-m}{m}\Big)\phi(-1) \qquad 0 \qquad \frac{1}{n}\frac{d\psi}{dz_2}(-1) \qquad 0$$

whereas into B_r we write

$$\frac{d\phi}{dz_1}(-1) \qquad 0 \qquad \frac{1}{n}\frac{d\psi}{dz_2}(-1) \qquad 0$$

To check the code we ran it with $R = 10^4, a = 1, m = n = 1, u_n = 0$ and we reproduce Orszag's [27] results, cf. section 2, although a "degenerate" interface eigenvalue of (1,0) is found. That this is acceptable follows from boundary condition $(6.13)_4$ where $c = 1$ is a solution.

Employing 150 polynomials in each of ϕ, ξ, ψ and ω we have made several calculations of spectra. Our choice of parameters was guided by Hooper's [19] results for the leading eigenvalue at criticality, i.e. the value of c between linear stability and instability for which $c_i = 0$. Her numerical technique was an orthonormalization type shooting method which locates one eigenvalue. We have not previously seen calculations of the spectra for the superposed fluids problem. Hooper [19] reports that for $m = 2, n = 1.2$ there are two distinct modes of possible instability if the Reynolds number is sufficiently high; one due to shear in the bulk of the fluids whereas the other is due to the interface effect. She reports that the orthonormalization technique could not determine the growth rates of the shear mode to sufficient accuracy. We have seen no trouble with this employing the method outlined here. In figure 18 we include the spectrum obtained for the parameter values $R = 10^4, u_n = 0, m = 2, n = 1.2, a = 1$, which is well into the shear instability zone of Hooper [19], which she reports begins around $R = 7400$. The shear mode is the one crossing the $c_i = 0$ axis at the upper left whereas the interface mode is the one in the top right corner. The splitting of the tail is not a numerical instability as we confirmed by calculation with 128 bit arithmetic. This feature is, in fact, observed as m increases from 1. The actual numerical values of the two leading eigenvalues in figure 18 are presented in table 5.

Mode Type	Eigenvalue c
interface	$1.003907431 + 0.1791888368E - 02i$
shear	$0.2578942002 + 0.8778915187E - 03i$

Table 5. Numerical values of the two leading eigenvalues in figure 18.

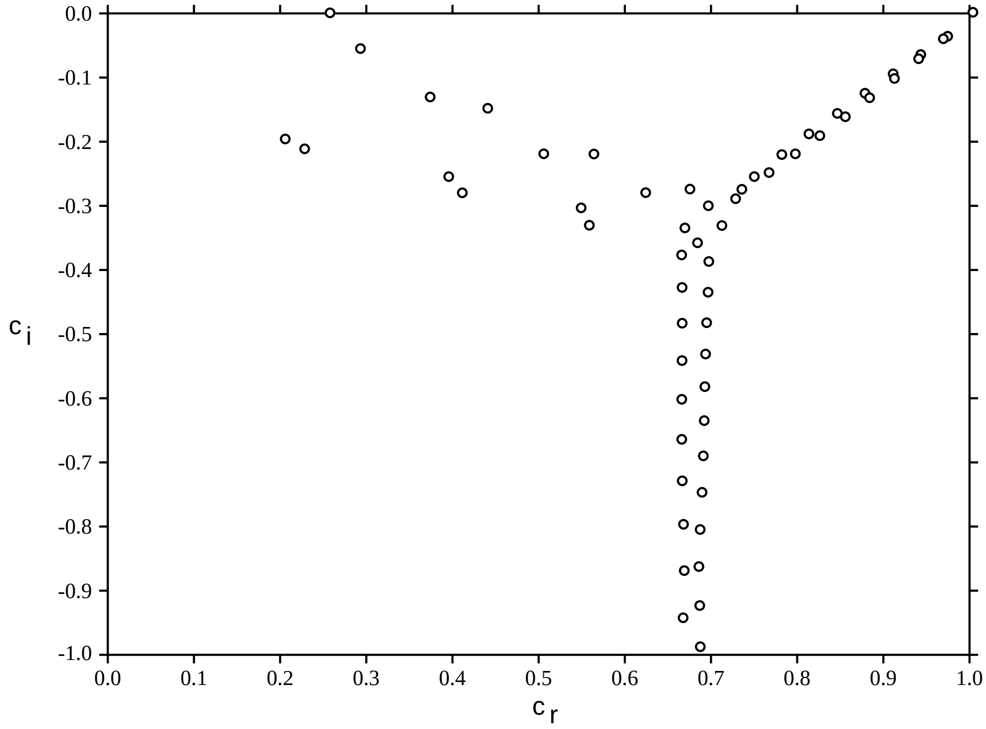

Figure 18 The spectrum for (6.11)-(6.13). $R = 10^4, a = 1, m = 2, n = 1.2, u_n = 0$.

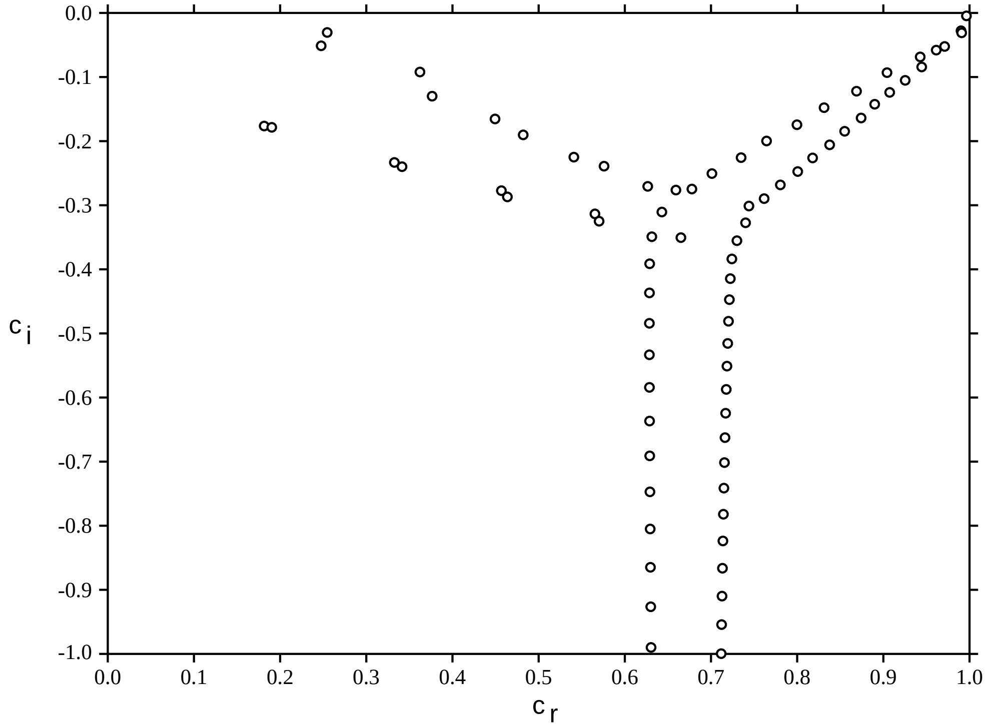

Figure 19 The spectrum for (6.11)-(6.13). $R = 10^4, a = 1, m = 2, n = 2, u_n = 0$.

Figure 19 shows how the tail splits more as n increases. Notice how for $n = 2$ the shear mode which is clearly unstable at $n = 1.2$ has dropped substantially into the stable zone. Hooper [19] reports that mode crossing occurs as n increases so the two separate modes which are unstable at $n = 1.2$ bifurcate at some intermediate value of n to form one stable mode when $n = 10$. Our investigations of various cases show the shear mode to be less influential when $n = 10$. For example, calculations with $n = 10, m = 2, u_n = 0, R = 500$ and $a = 0.37$ and $a = 4.5$ show one unstable mode, consistent with graph 5b of [19]; the $a = 4.5$ spectrum shows evidence of a shear like branch, but the leading eigenvalue of this branch is well into the stable zone.

We have three further mpeg movies which may be viewed by opening the following URL with a web browser

`http://www.epm.ornl.gov/~walker/eigenproblems.html`

These contain the parameter evolution of the spectrum of the Hooper [19] problem. The parametric studies are (a) $R = 200, a = 2, m = 2, u_n = 0$, with n going from 1.2 to 10 in steps of 0.1, which corresponds to a change from Hooper's [19] figure 5a to figure 5b; (b) $a = 1, u_n = 3, m = 2, n = 10$, with R going from 25 to 125 in steps of 1, which corresponds to figure 6b of [19]; (c) $R = 100, u_n = 2, m = 2, n = 10$, with a going from 0.3 to 2.3 in steps of 0.02, this corresponding to figure 6a of [19].

The "evolutionary" behaviour is revealing. In the (b) case we see only one leading mode which begins in the stable zone then becomes unstable before again returning to the stable zone, entirely consistent with the neutral curve of [19]. The eigenvalues "emanate" from two points on the $c_i = -1$ axis, one point just below $c_r = 1$ whereas the other is at approximately $c_r = 2.45$. The spectra for the extreme cases $R = 25$ and $R = 125$ are shown in figures 20 and 21.

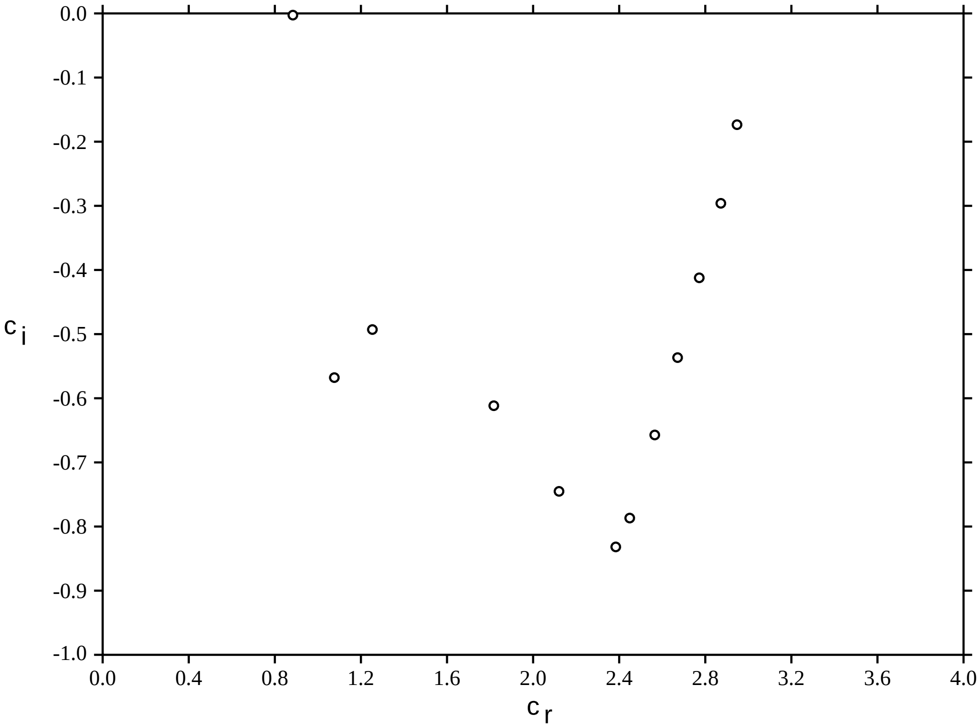

Figure 20 The spectrum for (6.11)-(6.13). $R = 25, a = 1, m = 2, n = 10, u_n = 3$.

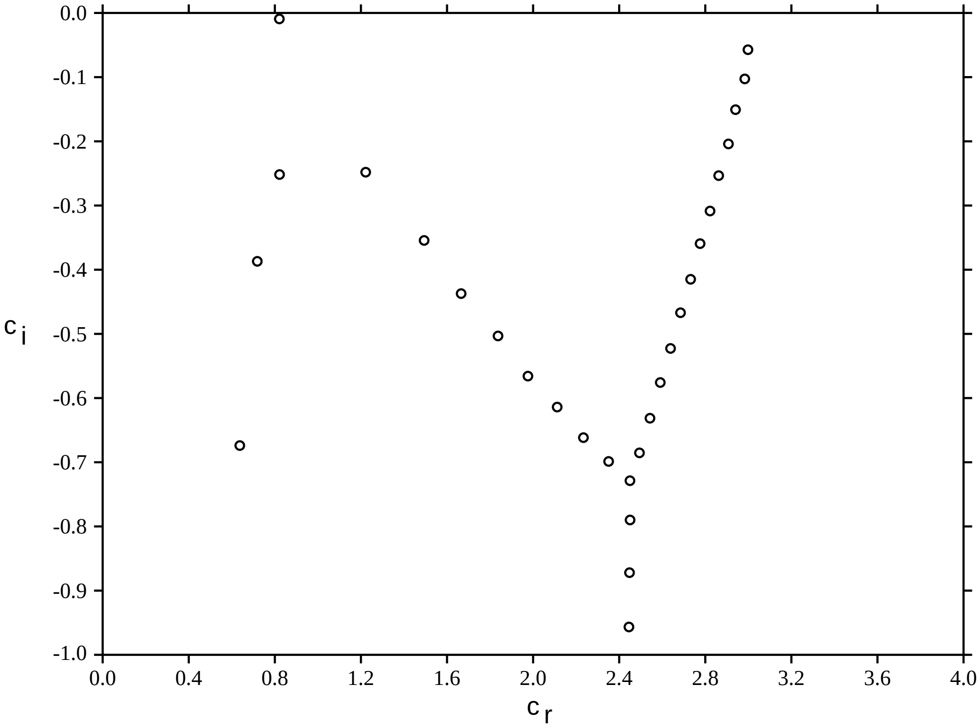

Figure 21 The spectrum for (6.11)-(6.13). $R = 125, a = 1, m = 2, n = 10, u_n = 3$.

The track in the wave number a, case (c), again shows one leading eigenvalue which begins in the stable region, goes unstable, then stable, and finally unstable, which again is consistent with the neutral curve in [19]. Again, the eigenvalues emanate from two places on the $c_i = -1$ axis, one of these being $c_r \approx 2.1$ while the other varies between $c_r \approx 0.8$ and $c_r \approx 0.6$. The cases $a = 0.3$ and $a = 2.3$ are displayed in figures 22 and 23.

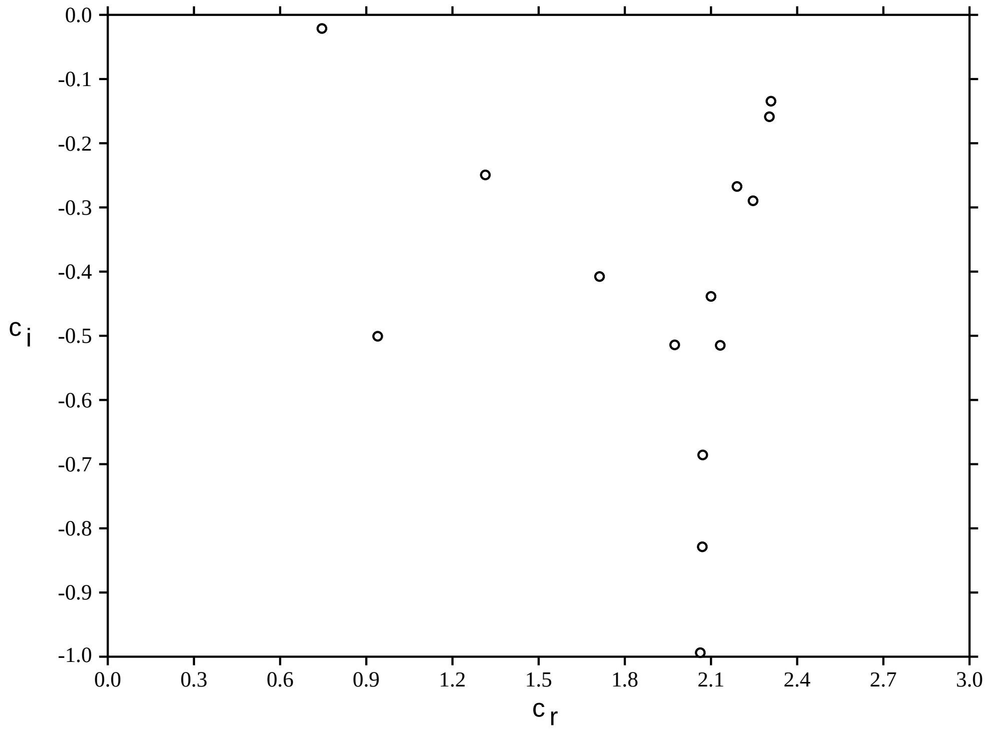

Figure 22 The spectrum for (6.11)-(6.13). $R = 100, a = 0.3, m = 2, n = 10, u_n = 2$.

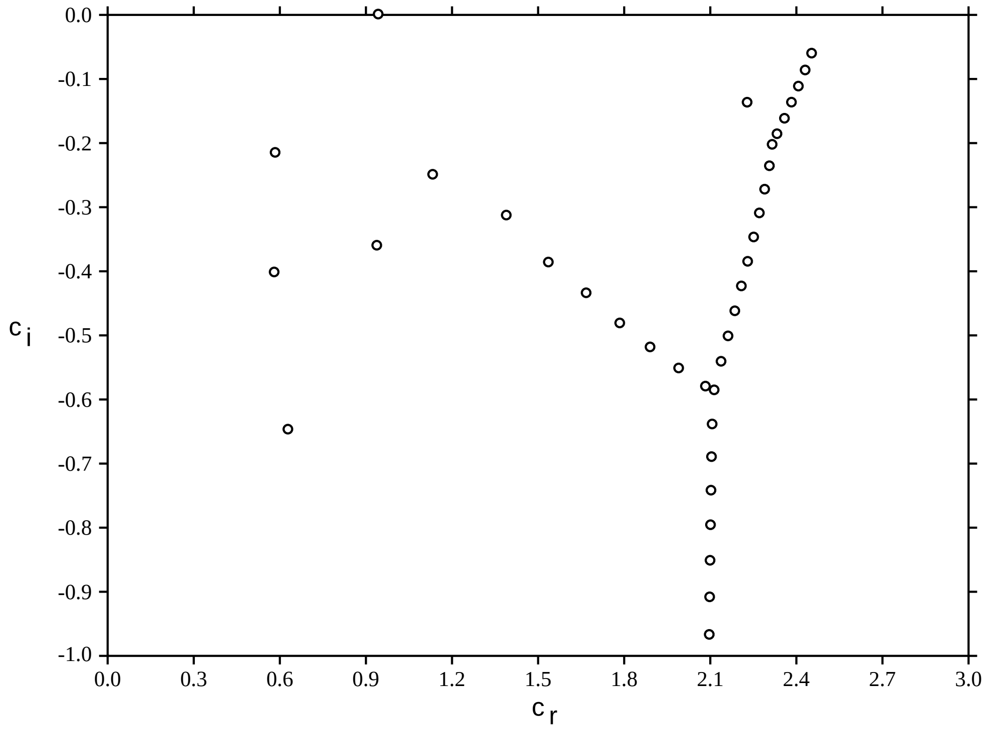

Figure 23 The spectrum for (6.11)-(6.13). $R = 100, a = 2.3, m = 2, n = 10, u_n = 2$.

Variation in n in the movie for case (a) is interesting. The leading eigenvalue begins unstable and finishes stable as n is varied from 1.2 to 10, consistent with the neutral curves of [19]. However, at $n \approx 2.9$ this eigenvalue moves sharply down into the stable region while an eigenvalue below moves sharply upward. To the resolution we have they appear to almost "bounce" off each other with the leading eigenvalue then going close to the $c_i = 0$ axis but remaining stable. Figure 24 shows this effect and numerical values of the two leading eigenvalues for n close to 2.9 are given in table 6. In this case the eigenvalues appear to emanate from only one point on the $c_i = -1$ axis. For n between 1.2 and 2.3 they come from $c_r \approx 0.67$ and at $n \approx 2.9$ this position of emanation begins to move rapidly to the right. Figure 25 displays the spectrum for $n = 10$. Those eigenvalues on the left side are left from the ones which came from below before $n \approx 2.7$. There is definite evidence of some transistion at $n \approx 2.9$, where several eigenvalues appear to "bounce" off each other. The two new branches coming from the main right branch begin to form at $n \approx 3.6$. Hooper's [19] comments on a transistion as n increases are consistent with what we have observed.

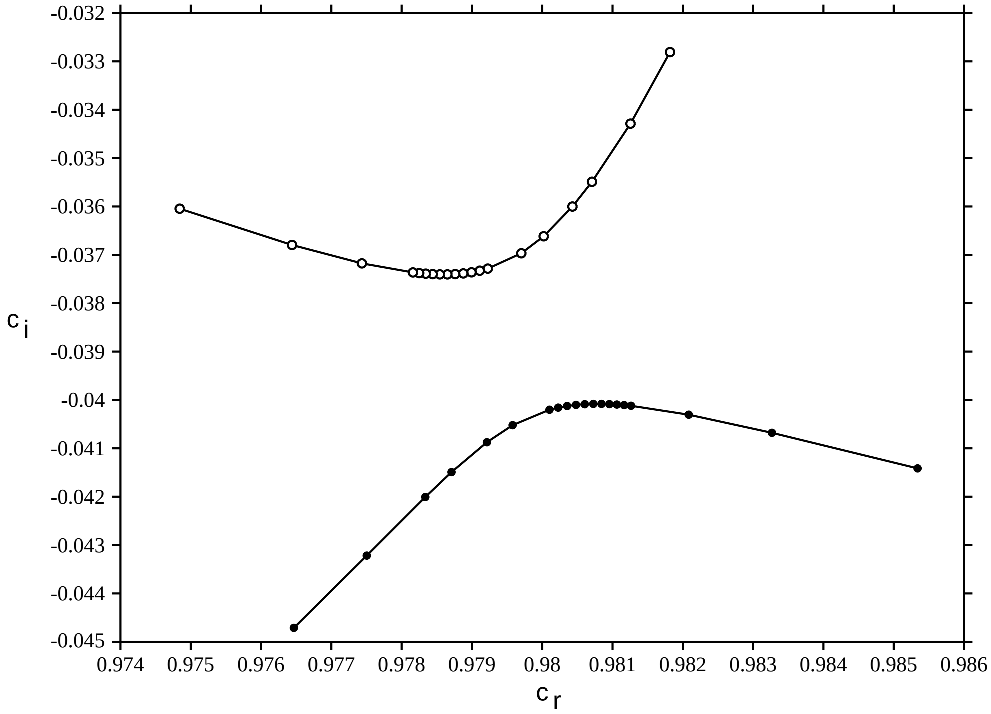

Figure 24 The behaviour of the two dominant eigenvalues for $n \approx 2.9$. $R = 200, a = 2, m = 2, u_n = 0$. The upper one ($\circ$) moves from upper right, lower one ($\bullet$) moves from lower left, for n increasing. Plots are for n =2.8900, 2.8950, 2.8980, 2.8990, 2.9000, 2.9005, 2.9010, 2.9011, 2.9012, 2.9013, 2.9014, 2.9015, 2.9016, 2.9017, 2.9018, 2.9019, 2.9020, 2.9030, 2.9050, 2.9100.

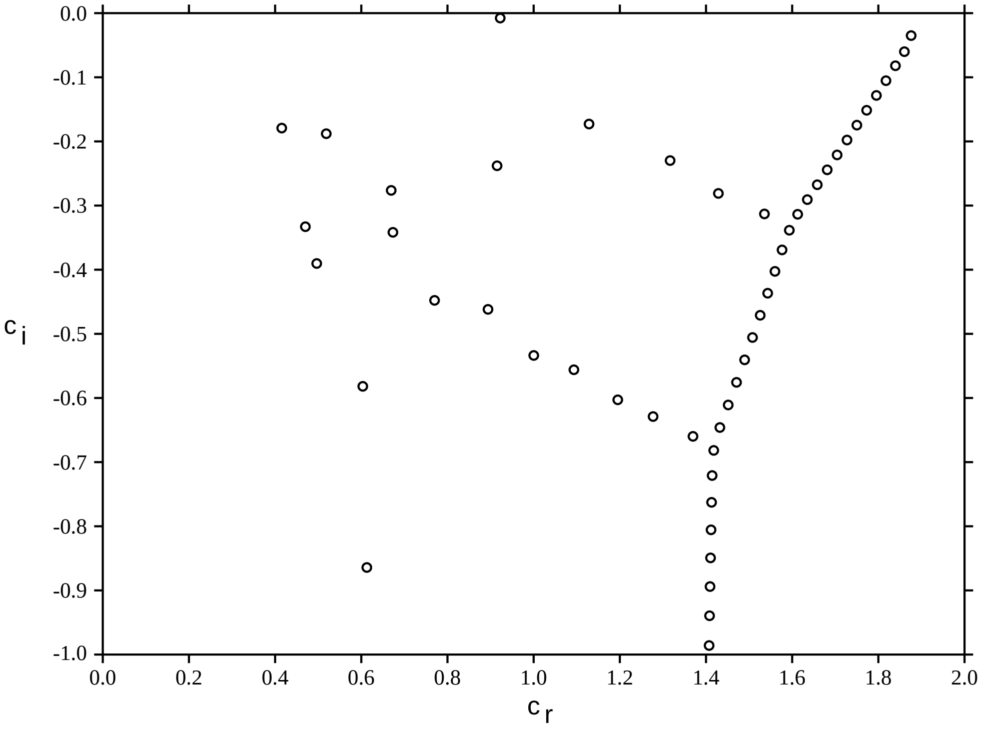

Figure 25 The spectrum for (6.11)-(6.13). $R = 200, a = 2, m = 2, n = 10, u_n = 0$.

Eigenvalue	$c^{(j)}$	n
0.9792258692E+00 -0.3728473376E-01	$c^{(1)}$	2.9010
0.9801031569E+00 -0.4020230541E-01	$c^{(2)}$	2.9010
0.9791112245E+00 -0.3732802803E-01	$c^{(1)}$	2.9011
0.9802272885E+00 -0.4015871356E-01	$c^{(2)}$	2.9011
0.9789940742E+00 -0.3736113699E-01	$c^{(1)}$	2.9012
0.9803539254E+00 -0.4012530718E-01	$c^{(2)}$	2.9012
0.9788769379E+00 -0.3738412623E-01	$c^{(1)}$	2.9013
0.9804805482E+00 -0.4010202060E-01	$c^{(2)}$	2.9013
0.9787619269E+00 -0.3739792636E-01	$c^{(1)}$	2.9014
0.9806050456E+00 -0.4008792331E-01	$c^{(2)}$	2.9014
0.9786504856E+00 -0.3740393958E-01	$c^{(1)}$	2.9015
0.9807259732E+00 -0.4008161315E-01	$c^{(2)}$	2.9015
0.9785434033E+00 -0.3740366471E-01	$c^{(1)}$	2.9016
0.9808425417E+00 -0.4008159114E-01	$c^{(2)}$	2.9016
0.9784409731E+00 -0.3739846465E-01	$c^{(1)}$	2.9017
0.9809544578E+00 -0.4008649443E-01	$c^{(2)}$	2.9017
0.9783431703E+00 -0.3738947637E-01	$c^{(1)}$	2.9018
0.9810617465E+00 -0.4009518618E-01	$c^{(2)}$	2.9018
0.9782497957E+00 -0.3737760251E-01	$c^{(1)}$	2.9019
0.9811646068E+00 -0.4010676365E-01	$c^{(2)}$	2.9019
0.9781605657E+00 -0.3736354301E-01	$c^{(1)}$	2.9020
0.9812633224E+00 -0.4012052694E-01	$c^{(2)}$	2.9020

Table 6. Numerical values of the two leading eigenvalues shown in figure 24.

Remarks. 1. The D^2 Chebyshev tau - QZ algorithm method extends to arbitrarily large systems which may be found, for example, in multi-component convection when many constituents are present and even chemical reactions are taking place, or in such a problem as thermal convection with Hall and ion slip currents simultaneously in effect; the latter problem is twelfth order even without flow effects, see Maiellaro *et al.* [24]. In this case very large systems of algebraic equations are encountered especially when the differential equations are stiff, or higher dimensions are considered, as in the plane Poiseuille or Couette flow problems coupled with effects such as multi-component diffusion and thermal convection, or Hall and ion slip MHD influences; such problems have a wide practical application, see e.g. Mulone [26]. For such classes of problem we see that the precision representation of a real number presents a difficulty. The D method of Lindsay & Ogden [21] would appear in some ways desirable because of the $O(M)$ growth of coefficients; however, the fact that the matrices are each of size $JM \times JM$ where J is the order of the system is a very severe restriction. To give an explicit example, the problem of thermal convection with two competing species as studied in [37] if coupled with Couette and / or Poiseuille flow, Hall and ion slip effects, in the case of one fluid overlying another would give rise to two 16th order systems and the resulting matrices in the D method would be $32M \times 32M$; if we require 200 polynomials for accurate resolution this means finding the eigenvalues of a 6400×6400 generalised matrix problem. Even a D^2 method for a large number of polynomials and extended precision calculation requires a large amount of memory and a long run time; the problem alluded to above would require 3200×3200 matrices for 200 polynomials. The very large matrix systems which will be encountered in stability studies on practical problems like that quoted above are precisely the domain for application of software libraries, such as ScaLAPACK Choi *et al.* [6], Dongarra *et al.* [9,10]. Unfortunately, however, at the time of writing a parallel version of the QZ algorithm is not yet available in the ScaLAPACK library. Another line of attack is to use the Arnoldi (iterative) method, see [6], and this will form part of future work.

2. As a further check on accuracy, we computed the sensitivities, Stewart & Sun [34], defined as

$$s^{(i)} = \frac{\|\mathbf{x}_i\|\|\mathbf{y}_i\|}{\mathbf{x}_i^H \mathbf{y}_i}$$

for the problem (1.1) with A and B defined as in this section; here $\mathbf{x}$ and $\mathbf{y}$ are right and left eigenvectors of (1.1), respectively. The absolute values for the first ten “eigenvalues” are given in table 7 below; the first three values computed are spurious eigenvalues. The quantity $\log_{10} s^{(i)}$ is a measure of the number of digits one loses in accuracy. It is seen that even in full precision (64 bit arithmetic) high accuracy is expected. The sensitivities for the three spurious eigenvalues are also of the same order as those appropriate to eigenvalues of the physical problem, which indicates that the spurious eigenvalues arise from the discretization, not the QZ algorithm.

Mode Number	Sensitivity	c_r	c_i
1	.104875E+05	.9306062397E-01	.5398774786E+05
2	.955170E+04	-.3477822923E+05	.6583840773E+04
3	.955169E+04	.3477831961E+05	.6583707360E+04
4	.192577E+05	.1008716826E+01	.8889416072E-03
5	.133748E+03	.6644993935E+00	-.1242776632E+00
6	.462979E+03	.7467618987E+00	-.1793830027E+00
7	.113398E+04	.7446257506E+00	-.2683049316E+00
8	.160433E+04	.7127003503E+00	-.3747130589E+00
9	.965561E+03	.6933402508E+00	-.5181828296E+00
10	.140640E+04	.6865584144E+00	-.7191848687E+00

Table 7. The sensitivities of the first ten computed "eigenvalues". $R = 100, a = 2, m = 2, n = 1.2, u_n = 0, M = 150$.

Acknowledgments. This research was supported in part by an appointment to the post-graduate research program at the Oak Ridge National Laboratory (ORNL) administered by the Oak Ridge Institute for Science and Education.

References

1. Abdullah, A.A. & Lindsay, K.A. Some remarks on the computation of the eigenvalues of linear systems. *Math. Models and Methods in Applied Sciences* **1** (1991), 153–165.

2. Anderson, E., Bai, Z., Bischof, C., Demmel, J., Dongarra, J.J., Du Croz, J., Greenbaum, A., Hammarling, S., McKenney, A., Ostrouchov, S. & Sorensen, D. *LAPACK Users' guide* (2nd Edition), SIAM (1995).

3. Butler, K.M. & Farrell, B.F. Three-dimensional optimal perturbations in viscous shear flow. *Phys. Fluids A* **4** (1992), 1637–1650.

4. Canuto, C., Hussaini, M.Y., Quarteroni, A. & Zang, T.A. 1988. *Spectral methods in fluid dynamics.* Springer - Verlag, Berlin - Heidelberg.

5. Chen, K.P. & Crighton, D.G. Instability of the large Reynolds number flow of a Newtonian fluid over a viscoelastic fluid. *Phys. Fluids A* **6** (1994), 152–163.

6. Choi, J., Dongarra, J.J., Pozo, R., Sorensen, D.C. & Walker, D.W. CRPC research into linear algebra software for high performance computers. *Int. J. Supercomputer Applications* **8** (1994), 99–118.

7. Davey, A. A simple numerical method for solving Orr-Sommerfeld problems. *Q. Jl. Mech. Appl. Math.* **26** (1973), 401–411.

8. Davey, A. & Drazin, P.G. The stability of Poiseuille flow in a pipe. *J. Fluid Mech.* **36** (1969), 209–218.

9. Dongarra, J.J., van de Geijn, R.A. & Walker, D.W. Scalability issues affecting the design of a dense linear algebra library. *J. Parallel and Distributed Computing* **22** (1994), 523–537.

10. Dongarra, J.J. & Walker, D.W. Software libraries for linear algebra computations on high performance computers. *SIAM Review,* to appear.

11. Drazin, P.G. & Reid, W.H. *Hydrodynamic stability.* Cambridge University Press (1981).

12. Fearn, D.R. Eigensolutions of boundary value problems using inverse iteration. *J. Comp. Appl. Math.* **34** (1991), 201–209.

13. Gardner, D.R., Trogdon, S.A. & Douglas, R.W. A modified tau spectral method that eliminates spurious eigenvalues. *J. Computational Physics* **80** (1989), 137–167.

14. Gustavsson, L.H. Resonant growth of three-dimensional disturbances in plane Poiseuille flow. *J. Fluid Mech.* **112** (1981), 253–264.

15. Gustavsson, L.H. & Hultgren, L.S. A resonance mechanism in plane Couette flow. *J. Fluid Mech.* **98** (1980), 149–159.

16. Haidvogel, D.B. & Zang, T. The accurate solution of Poisson's equation by expansion in Chebyshev polynomials. *J. Computational Phys.* **30** (1979), 167–180.

17. Henningson, D.S. & Reddy, S.C. On the role of linear mechanisms in transition to turbulence. *Phys. Fluids* **6** (1994), 1396–1398.

18. Herbert, T. *Die neutrale fläche der ebenen Poiseuille - Strömung.* Habilitation, Universität Stuttgart (1977).

19. Hooper, A.P. The stability of two superposed viscous fluids in a channel. *Phys. Fluids A* **1** (1989), 1133–1142.

20. Huang, W. & Sloan, D.M. The pseudospectral method for solving differential eigenvalue problems. *J. Computational Phys.* **111** (1994), 399–409.

21. Lindsay, K.A. & Ogden, R.R. A practical implementation of spectral methods resistant to the generation of spurious eigenvalues. *Int. J. Numer. Methods Fluids* **15** (1992), 1277–1294.

22. McFadden, G.B., Murray, B.T. & Boisvert, R.F. Elimination of spurious eigenvalues in the Chebyshev tau spectral method. *J. Computational Physics* **91** (1990), 228–239.

23. Mack, L.M. A numerical study of the temporal eigenvalue spectrum of the Blasius boundary layer. *J. Fluid Mech.* **73** (1976), 497–520.

24. Maiellaro, M., Palese, L. & Labianca, A. Instabilizing - stabilizing effects of MHD anisotropic currents. *Int. J. Engng. Sci.* **27** (1989), 1353–1359.

25. Moler, C.B. & Stewart, G.W. An algorithm for generalized matrix eigenproblems. *SIAM. J. Numerical Anal.* **10** (1973), 241–256.

26. Mulone, G. On the nonlinear stability of a fluid layer of a mixture heated and salted from below. *Continuum Mech. Thermodyn.* **6** (1994), 161–184.

27. Orszag, S.A. Accurate solution of the Orr - Sommerfeld stability equation. *J. Fluid Mech.* **50** (1971), 689–703.

28. Reddy, S.C. & Henningson, D.S. Energy growth in viscous channel flows. *J. Fluid Mech.* **252** (1993), 209–238.

29. Reddy, S.C., Schmid, P.J. & Henningson, D.S. Pseudospectra of the Orr-Sommerfeld operator. *SIAM J. Appl. Math.* **53** (1993), 15–47.

30. Renardy, Y. Weakly nonlinear behaviour of periodic disturbances in two-layer Couette-Poiseuille flow. *Phys. Fluids A* **1** (1989), 1666–1676.

31. Rionero, S. & Mulone, G. On the nonlinear stability of parallel shear flows. *Continuum Mech. Thermodyn.* **3** (1991), 161–184.

32. Schmid, P.J. & Henningson, D.S. Optimal energy density growth in Hagen-Poiseuille flow. *J. Fluid Mech.* **277** (1994), 197–225.

33. Shanthini, R. Degeneracies of the temporal Orr-Sommerfeld eigenmodes in plane Poiseuille flow. *J. Fluid Mech.* **201** (1989), 13–34.

34. Stewart, G.W. & Sun, J.-G. *Matrix Perturbation Theory*, Academic Press, New York (1990).

35. Straughan, B. & Walker, D.W. Anisotropic porous penetrative convection. *Proc. Roy. Soc. London A*, to appear.

36. Straughan, B. & Walker, D.W. Two very accurate and efficient methods for computing eigenvalues and eigenfunctions in porous convection problems. To appear.

37. Straughan, B. & Walker, D.W. Multi-component diffusion, non-Boussinesq convection, and the Chebyshev tau method. To appear.

38. Trefethen, L.N., Trefethen, A.E. & Reddy, S.C. Pseudospectra of the linear Navier-Stokes evolution operator and instability of plane Poiseuille and Couette flows: (preliminary report). *Tech. Report* **92-1291**, Dept. Computer Science, Cornell University (1992).

39. Yih, C.S. Instability due to viscosity stratification. *J. Fluid Mech.* **27** (1967), 337–352.

40. Zebib, A. Removal of spurious modes encountered in solving stability problems by spectral methods. *J. Computational Phys.* **70** (1987), 521–525.